

**IZMIR KATIP CELEBI UNIVERSITY
GRADUATE SCHOOL OF NATURAL AND APPLIED SCIENCES**

**AN INVESTIGATION OF LEAKAGE DEFECTS' REPAIR OF ALUMINIUM
CASTED PARTS BY USING LOW PRESSURE COLD SPRAY METHOD**

M.Sc. THESIS

Samet YILMAZ

Department of Materials Science and Engineering

JULY 2019

**IZMIR KATIP CELEBI UNIVERSITY
GRADUATE SCHOOL OF NATURAL AND APPLIED SCIENCES**

**AN INVESTIGATION OF LEAKAGE DEFECTS' REPAIR OF ALUMINIUM
CASTED PARTS BY USING LOW PRESSURE COLD SPRAY METHOD**

M.Sc. THESIS

**Samet YILMAZ
Y130111039**

Department of Materials Science and Engineering

Thesis Advisor: Prof. Dr. M. Özgür SEYDİBEYOĞLU

JULY 2019

İZMİR KATİP ÇELEBİ ÜNİVERSİTESİ
FEN BİLİMLERİ ENSTİTÜSÜ

SIZDIRMA HATASI BULUNAN ALÜMİNYUM DÖKÜM PARÇALARININ
ALÇAK BASINÇLI SOĞUK SPREY METODU İLE GERİ KAZANIMI

YÜKSEK LİSANS TEZİ

Samet YILMAZ
Y130111039

Malzeme Bilimi ve Mühendisliği Ana Bilim Dalı

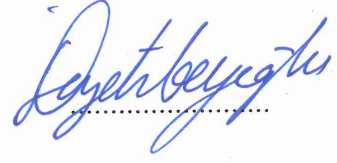
Tez Danışmanı: Prof. Dr. M. Özgür SEYDİBEYOĞLU

TEMMUZ 2019

Samet YILMAZ, a M.Sc. student of IKCU Graduate School Of Natural And Applied Sciences, successfully defended the thesis entitled “AN INVESTIGATION OF LEAKAGE DEFECTS’ REPAIR OF ALUMINIUM CASTED PARTS BY USING LOW PRESSURE COLD SPRAY METHOD”, which he prepared after fulfilling the requirements specified in the associated legislations, before the jury whose signatures are below.

Thesis Advisor :

**Prof. Dr. M. Özgür
SEYDİBEYOĞLU**
İzmir Katip Çelebi University

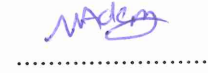


Jury Members :

**Assoc. Prof. Mücahit
SÜTÇÜ**
İzmir Katip Çelebi University



**Asst. Prof. Umut
ADEM**
İzmir Institute of Technology



Date of Submission : 26.06.2019

Date of Defense : 26.07.2019

To my family,

FOREWORD

First and foremost, I would like to thank my advisor, M. Özgür SEYDİBEYOĞLU for his patience, support, guidance and insight through the project.

This thesis was supported by Izmir Katip Celebi University, Coordination Office of Scientific Research Projects and Mechanical Engineering Department. Special thanks to Ebubekir ATAN for their support for using Dymet 423 LPCS equipment.

I owe a great debt of gratitude to my supportive and encourager colleagues Emre KOCA and Daryal İNCE. They provided me full support from beginning to end. Additional thanks to Nazan AYSAN for her belief in my success and being a best motivator.

Finally, I would like to thank my precious family. They are the best luck of my life. I owe to them all my success and opportunities in my life.

July 2019

Samet YILMAZ

TABLE OF CONTENTS

	<u>Page</u>
FOREWORD	v
TABLE OF CONTENTS	vi
ABBREVIATIONS	viii
LIST OF TABLES	ix
LIST OF FIGURES	x
ABSTRACT	xii
ÖZET	xiii
1. INTRODUCTION	1
2. ALUMINIUM AND ALUMINUM ALLOYS	3
2.1 Aluminium Alloys.....	4
2.1.1 A356 Aluminium Alloy	5
2.2 Alloying Elements.....	7
2.2.1 Copper.....	8
2.2.2 Silicon	8
2.2.3 Magnesium.....	8
2.2.4 Strontium.....	9
2.2.5 Titanium	10
2.2.6 Boron.....	10
2.2.7 Iron	10
2.3 Low Pressure Die Casting of A356 Alloy Wheels.....	11
2.4 Casting Defects During A356 Wheel Production	14
2.4.1 Defects Due to Alloy.....	14
2.4.2 Defects Due to Melting	15
2.4.3 Defects Due to Casting	16
2.4.3.1 Oxides (Bifilm)	17
2.4.3.2 Porosity	18
2.4.3.3 Leakage Defetcts	19
3. COLD SPRAY	20
3.1 History of Cold Spray	20
3.2 Areas of Usage	22
3.3 Main Components and Basic Process Description.....	23
3.4 High Pressure Cold Spray	27
3.5 Low Pressure Cold Spray	28
4. EXPERIMENTS	32
4.1 Material and Method	32
4.2 Experiments for Optimum Parameter	35
4.3 Experimental Procedure for Leakage Defect Coating.....	36
5. RESULTS AND DISCUSSIONS	40
5.1 Powder Characterization and Parameter Experiments Results	40

5.2 X-ray Control Results.....	47
5.3 Microstructure Investigation Results	48
5.4 Hardness Test Results	48
5.5 90° Impact Test Results.....	49
5.6 Radial Fatigue Test Results.....	50
6. CONCLUSION.....	52
REFERENCES	54
APPENDIX	56
CURRICULUM VITAE.....	59

ABBREVIATIONS

ANSI	: American National Standards Institute
LPDC	: Low Pressure Die Casting
GDC	: Gravity Die Casting
A356	: Aluminium Casting Alloy
Mg ₂ Si	: Magnesium Silicide
Al ₂ B	: Aluminium Boride
TiB ₂	: Titanium Diboride
TiAl ₃	: Titanium Aluminide
AlTi ₅ B ₁	: Aluminium Titanium Boron
CrC	: Chromium Carbide
NiCr	: Nickel Chromium
WC-Co	: Tungsten Carbide Cobalt
WCu	: Tungsten Copper
V _p	: Particle Velocity
V _c	: Critical Velocity
HVPC	: High Velocity Particle Consolidation
SPD	: Supersonic Particle/Powder Deposition
Al ₂ O ₃	: Alumina
μm	: Micronmeter
HPCS	: High Pressure Cold Spray
LPCS	: Low Pressure Cold Spray
SEM	: Scanning Electron Microscope
EDS	: Energy Dispersive Spectrometry
D _v	: Size Distribution Values
HB	: Hardness Brinell
kN	: Kilonewtons

LIST OF TABLES

	<u>Page</u>
Table 2.1 : Aluminium Foundry Alloys [4]	4
Table 2.2 : Chemical Composition of Aluminium Alloys	6
Table 2.3 : Mechanical Properties of A356 Alloy	7
Table 2.4 : Inclusion types and root causes.....	16
Table 5.1 : EDS analysis of K-20-11	40
Table 5.2 : EDS analysis of SST-A5006.....	41
Table 5.3 : Coating thicknesses according temperature and feeding rate	43
Table 5.4 : EDS analysis of K-20-11 coating on A356 alloy wheel (3 rd temperature level, 6 th feeding rate level).....	44
Table 5.5 : EDS analysis of SST-A5006 coating on A356 alloy wheel (5 th temperature level, 7 th feeding rate level).....	46
Table 5.6 : Hardness measurements after painting process	49
Table 5.7 : Wheel Model.1 90° Impact Test Results	50
Table 5.8 : Wheel Model.2 90° Impact Test Results	50
Table 5.9 : Penetration test results for crack existence after radial fatigue test	51

LIST OF FIGURES

	<u>Page</u>
Figure 2.1 : Bauxite mineral resources around the world [2]	3
Figure 2.2 : Al-Si phase diagram and aluminium alloys [2].....	8
Figure 2.3 : Mg ₂ Si precipitation in AlSi alloy according to temperature [2]	9
Figure 2.4 : a) not modified microstructure b) modified microstructure after Sr addition [2]	10
Figure 2.5 : Iron content in AlSi alloys a) Needle β -Al ₅ FeSi b) Chinese script α - Al ₈ Fe ₂ Si c) π-Al ₈ FeMg ₃ Si ₆ [2]	11
Figure 2.6 : Schematic drawing of reverberatory furnace [6].....	12
Figure 2.7 : Schematic drawing of reverberatory furnace [9].....	13
Figure 2.8 : Schematic drawing of LPDC system [12]	14
Figure 2.9 : Corundum formation [13]	15
Figure 2.10 : Formation of oxide films [13]	18
Figure 2.11 : Shapes of shrinkage, hydrogen and air porosity [13]	19
Figure 2.12 : Leakage defect on rim surface.....	19
Figure 3.1 : First patented cold spray device [19].....	21
Figure 3.2 : First portable cold spray gun [19]	21
Figure 3.3 : a) Corroded T-6 Aircraft Wheel b) After Cold Sprayed T-6 Aircraft Wheel [21].....	22
Figure 3.4 : a) Magnesium Casting Defect b) Cold Sprayed Repair Casting [21] ...	23
Figure 3.5 : Restoration of an old sculpture by cold spray method [22].....	23
Figure 3.6 : Cold spray process formation levels [25].....	24
Figure 3.7 : Schematic diagram of the cold spray SST Centerline system [23]	25
Figure 3.8 : Corelation between Standoff distance and deposition efficiency [26]..	26
Figure 3.9 : Corelation between Gas temperature and % porosity in Cu based coating [27]	27
Figure 3.10 : Schematic diagram of HPCS system [23]	28
Figure 3.11 : Image of commercial stationary HPCS system [27]	28
Figure 3.12 : Schematic diagram of LPCS system [23].....	29
Figure 3.13 : Commercial LPCS equipmet and automated spraying gun system [22]	29
Figure 4.1 : Dymet 423 LPCS equipment.....	32
Figure 4.2 : Carl Zeiss 300VP SEM	33
Figure 4.3 : Malvern Master Sizer 3000	34
Figure 4.4 : Nikon Eclipse MA 100 with Clemex Image Analyses System.....	34
Figure 4.5 : Bosello WRE Thunder 3 X-Ray System.....	35
Figure 4.6 : a) Blasted rim surface with K-00-04-16 b) Coated rim surface with K- 20-11	36
Figure 4.7 : Some examples of leakage defect areas on rim surface	37
Figure 4.8 : Some examples of coated leakage defect areas on rim surface.....	38

Figure 4.9 : A wheel that has leakage defect	38
Figure 5.1 : SEM image of K-20-11	40
Figure 5.2 : Particle size distribution of K-20-11 (Dv (10) 7,31 μm , Dv (50) 21,4 μm Dv (90) 43,3 μm)	41
Figure 5.3 : SEM image of SST-A5006.....	41
Figure 5.4 : Particle size distribution of SST-A5006 (Dv (10) 7,63 μm , Dv (50) 23,2 μm Dv (90) 46,9 μm).....	42
Figure 5.5 : Microstructure under optical microscope of 3 rd temperature and 6 th feeding rate level (Optimum Condition).....	42
Figure 5.6 : SEM image of K-20-11 coating on A356 alloy wheel (3 rd temperature level, 6 th feeding rate level).....	44
Figure 5.7 : Coating problems during high feeding rate a) 4 th Temperature and 10 th feeding rate level b) 5 th temperature and 9 th feeding rate level c) 5 th temperature and 10 th feeding rate level	45
Figure 5.8 : SEM image of SST-A5006 coating on A356 alloy wheel (5 th temperature level and 7 th feeding rate level).....	46
Figure 5.9 : X-ray images of rim surface a) After coating process-excessive material on rim surface b) After grinding process-smooth rim surface	47
Figure 5.10 : Microstructures of coated wheel with K-20-11 a) After coating process b) After grinding process	48
Figure 5.11 : Measurement zones for cross section Hardness Test	49
Figure 5.12 : Schematic drawing of 90° Impact Test Equipment.....	50
Figure 5.13 : Schematic drawing of radial fatigue test equipment	51

AN INVESTIGATION OF LEAKAGE DEFECTS' REPAIR OF ALUMINIUM CASTED PARTS BY USING LOW PRESSURE COLD SPRAY METHOD

ABSTRACT

Nowadays Aluminium alloys and products are mostly used in automotive nowadays industry because of their light weight, durability and corrosion resistance. Aluminium alloys were found that they decrease the vehicle weight a lot and reduce the fuel consumption. Instead of using steel parts in the past, automotive manufacturers decided to use aluminium alloys for this reason. Lightweight aluminium alloys are generally manufactured by casting, extrusion and cold working methods. When body parts, chassis frames are mostly manufactured by extrusion, engine blocks and wheels are manufactured by casting methods.

As in various production method, there are kinds of defect types which can be occurred in aluminium casting. These defects are generally defined as scrap and recycled by re-melting. This situation creates "poor quality costs" and decreases profit margin of the company and effects environment negatively because of extra energy consumption. Low cost recovery methods are investigated instead of re-melting process for aluminium wheels which include surface defects such as leakage.

Low pressure cold spray is a low cost method and this kind of defect can be repaired with similar aluminium alloy powder. The main purpose of this research is to repair of leakage defects and to reduce poor quality costs by using LPCS method.

SIZDIRMA HATASI BULUNAN ALÜMİNYUM DÖKÜM PARÇALARININ ALÇAK BASINÇLI SOĞUK SPREY METODU İLE GERİ KAZANIMI

ÖZET

Günümüzde hafif, mukavemetli ve yüksek korozyon direncine sahip olması sebebiyle özellikle otomotive sektöründe alüminyum esaslı parçalar kullanılmaktadır. Eskiden ağırlıklı olarak çelik parçalar kullanılan otomotiv üreticileri üretimi ve işleme daha kolay olan ayrıca binek aracın ağırlığını çok ciddi oranda düşürerek yakıt tasarrufu da sağlayacak alüminyum alaşımları üzerine yönelmişlerdir. Ülkemizde gelişen otomotiv yan sanayide alüminyum esaslı parçalar döküm, ekstrüzyon ve soğuk şekil verme gibi yöntemlerle yüksek oranda üretilmektedir. Genellikle gövde parçaları, şasi ve kafes profilleri ekstrüzyon ile üretilirken motor blokları ve jantlar çeşitli döküm yöntemleri ile üretilir.

Her üretim yönteminde olduğu gibi döküm ile üretilmiş alüminyum esaslı parçalarda da birçok hata oluşmakta ve ürünler fire olarak ayrılmaktadır. Bu firelerin tekrar ergitilerek geri kazanılmaktadır. Bu durum kalitesizlik maliyeti oluşturarak hem şirketlerin kâr marjına hem de fazladan enerji kullanımı sebebiyle çevreye olumsuz yönde etkiler yapmaktadır. Özellikle jant gibi ürünlerin lastik yüzeyinde meydana gelen meydana gelen sızdırma hataları tekrar ergitilerek geri kazanım yerine daha düşük maliyetli geri kazanım yolları araştırılmıştır.

Çok düşük maliyetli bir yöntem olan alçak basınçlı soğuk sprej metodu ve dökümde kullanılan benzer bir alaşımlı toz ile bu tip hatalar tamir edilebilir. Bu araştırma kapsamında öncelikli olarak ince kesitlerde meydana gelen sızdırma hatalarının soğuk sprej yöntemiyle giderilmesi ve kalitesizlik maliyetinin azaltılması amaçlanmıştır.

1. INTRODUCTION

Aluminium has been discovered in 1836 but it could be produced at the end of 19th century. It is not found as a pure metal in nature for this reason it took a while to discover. Even though late discover, it is produced more than other non-ferrous metal total production amount in these days. It is also known as 8% of earth is covered with Al and it is 3rd mostly found element in the world. But generally it is located as oxidized and combined with other elements in earth.

Aluminium and aluminium alloys usage decreases gradually in automotive, aviation and aerospace industry. It became very strategic material in industrial areas because of its lightweight, corrosion resistance and good mechanical properties. Additionally, low melting temperature of aluminium provides easier manufacturing methods and less energy consumption than other structural materials such as steel. Although steel was the most common material in automotive industry, aluminium took its place long time ago.

After using many years in aviation and aerospace industry, aluminium and its alloys started to use in automotive industry for energy saving concerns. As a rough calculation aluminium is almost lighter 3 times than steel. Every 10% weight decrease of vehicle provides 6-7% fuel consumption saving. Overall aluminium usage in one vehicle instead of steel makes approximately 20% decrease of weight. Primary parts of vehicle can be produced as aluminum are engine blocks, body plates and frames and wheels.

High production amount creates more scrap. Aluminium is one of the easiest recoverable elements. Energy consumption of secondary production is just 5% of primary production. Although aluminium recovery is easy and cheap than the others, there is large energy consumption because of large amount of scrap ratio. In today's world, where the technological developments increase at great pace, it is very important to ensure to harmony of environment and technology for a livable world.

For this reason energy and fuel consumption should be decreased significantly. Before aluminium recovery and recycling, less scrap production should be considered.

For these concerns, aluminium scraps are desired to recover without re-melting in this study. Lightweight aluminium alloys are mostly in used for wheels for vehicles. Generally wheels are casted by low pressure casting machines. Producers face many casting defects during wheel manufacturing. The main defects in casting process are leakage, gas holes, shrinkage and porosity. These defects can be detected after machining process. Every process creates additional cost and re-melting every piece after any defect detection means loss of all costs for producers.

Low pressure cold spray is very easy to use and economic tool for repair and restoration processes. Ductile and soft powders such as aluminium, copper, tin and zinc can be easily coated onto metal substrate by low pressure cold spray without any heat and inert gas. Because it is very small and mobile unit, it can be easily used in every place that is desired. In this thesis, it is aimed to recover leakage casting defects by using low pressure cold spray method with using similar aluminium alloy powders.

2. ALUMINIUM AND ALUMINUM ALLOYS

At first in 1807, English scientist Sir Humphry Davy mentioned as “Alum is a salt of unknown metal” and called as “Alumium”. Continuous scientists called this metal as “Aluminium” [1].

After Davy’s experiments, Hans Christian Oersted heated potassium amalgam with aluminium chloride and collected little aluminium particles. In 1845, Wöhler determined many properties of this metal. Low density was the one of these determined properties [3].

Aluminium is the third most abundant element and metal in the earth crust (~8-13%). It is normally found in combination with oxygen and silicon. Oxide forms or silicates are such as bauxite, kaolinite, nepheline and alunite. Generally it is found at South America, Australia, Africa, Asia and Europe (Figure 2.1).

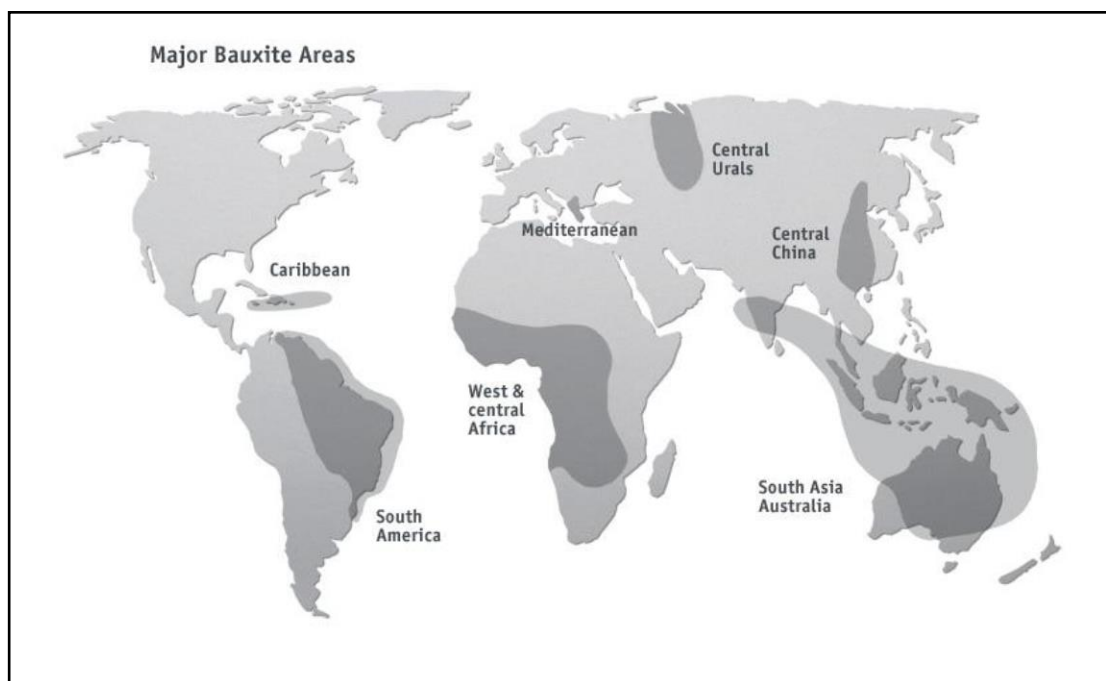


Figure 2.1 : Bauxite mineral resources around the world [2].

In 1886, Charles Martin Hall and Paul L.T. Heroult succeeded at producing aluminium by aluminium oxide electrolyte. Hall in USA, Heroult in France got patent and this

invention had a big effect on industry. After Hall-Heroult success, in 1888 Karl Bayer produced alumina from bauxite mineral. After 1890, aluminium price decreased less than %80 because of Da'ville method and it became commercial [1].

2.1 Aluminium Alloys

Mechanical, physical and chemical properties of aluminium alloys depend on alloying elements and microstructure. Major alloying elements for aluminium are such as: copper, manganese, silicon, magnesium and zinc. Aluminium alloys divided two different groups as forging and casting alloys. Forging alloys has very high deformation resistance for this reason they are easy to forge and form. Heat treatment can be applied to major part of forging and casting alloys.

General alloying and combinations of elements are given as number series in the ANSI coding system (Table 2.1).

Table 2.1 : Aluminium Foundry Alloys [4].

Number Series	Alloy Type
1XX.X	99.0% minimum aluminum content
2XX.X	Al + Cu
3XX.X	Al + Si & Mg, or Al + Si & Cu, or Al + Si & Mg & Cu
4XX.X	Al + Si
5XX.X	Al + Mg
7XX.X	Al + Zn
8XX.X	Al + Sn

Casting aluminum alloys are designated by a 3 digit number and a decimal point separating the 4th digit. The first digit mentions the alloy group in regards to the main alloying element. The 2nd and 3rd digit mean different. The last digit means the production type. If it is 0, it means casting. If it is 1 or 2, it means ingot. An alloy modification or impurity limitations is mentioned by a letter before the numerical series. Some differences exists for the first group (pure Al/1xx series).

The temper designation is separated from the alloy designation by a dash and indicates mechanical or thermal treatment. Additional digits to the right indicate variations in basic treatment.

F : As fabricated

O : Annealed (to improve ductility and dimensional stability).

H : Strain Hardened (products strengthened through cold-working). The “H” is always followed by two or more digits.

W : Solution Heat-Treated (applicable only to alloys which age spontaneously at room temperature after solution heat treatment).

T : Thermally Treated. It is always followed by one or more digits.

2.1.1 A356 aluminium alloy

A356 is one of hypo eutectic Al-Si alloys and it has a large field of application in the avionics and automotive industries. It is generally used as heat treated because of obtaining optimum mechanical properties. Castings that have non dendritic microstructure with low porosity and with good physical and mechanical properties are possible to achieve [5].

A356 is at the moment the most popular alloy of aluminum castings and partly solid metal manufacturing. A356 alloys are used for a kind of commercial castings too such as electrical and marine equipments, pump cases and etc. In USA, this alloy has been used as a material of automobile wheels and it has been started to use for chassis and suspensions as well [4]. In this study, A356 aluminium wheels will be used for a substrate.

Chemical composition of A356 alloy is given in Table 2.2 and mechanical properties are given in Table 2.3.

Table 2.2 : Chemical Composition of Aluminium Alloys

Alloy	% Si	% Cu	% Mn	% Mg	% Zn	% Ti	% Other
201.0	0,1 max	4,0-5,2	0,2-0,5	0,15-0,55	-	0,15-0,35	Ag 0,4-1,0
208.0	2,5-3,5	3,5-4,5	0,5 max	0,1 max	1,0 max	0,25 max	-
222.0	2,0 max	9,2-10,7	0,5 max	0,05-0,5	1,0 max	0,25 max	-
333.0	8,0-10,0	3,0-4,0	0,5 max	0,05-0,5	1,0 max	0,25 max	-
356.0	6,5-7,5	0,25 max	0,35 max	0,20-0,45	0,35 max	0,25 max	-
413.0	11,0-13,0	1,0 max	0,35 max	0,1 max	0,5 max	0,25 max	-
443.0	4,5-6,0	0,6 max	0,5 max	0,05 max	0,5 max	0,25 max	-
514.0	0,35 max	0,15 max	0,35 max	3,5-4,5	0,15 max	0,25 max	-
518.0	0,35 max	0,25 max	0,35 max	7,5-8,5	0,15 max	-	-
705.0	0,20 max	0,20 max	0,4-0,6	1,4-1,8	2,7-2,2	0,25 max	Cr 0,2-0,4
713.0	0,25 max	0,4-1,0	0,6 max	0,2-0,5	7,0-8,0	0,25 max	-
852.0	0,4 max	1,7-2,3	0,1 max	0,6-0,9	-	0,25 max	Sn 5,5-7,0 Ni 0,9-1,0

Table 2.3 : Mechanical Properties of A356 Alloy

Density (g/cm ³)	2,685
Liquidus Temperature (°C)	615
Solidus Temperature (°C)	555
0.2 % Proof Stress (N/mm ²)	185
Tensile Stress (N/mm ²)	230
Elongation (%)	2
Brinell Hardness (HB)	75
Endurance Limit	56
Modulus of Elasticity (N/m ²)	71
Shear Strength (N/m ²)	120

2.2 Alloying Elements

Alloying elements can be added by direct introduction and master alloys. Direct introduction elements have usually lower melting point lower aluminum and also Si. Master alloys are usually binary alloys containing the maximum percentage of the alloying element.

Alloying elements can be classified as primary, secondary, modifying or impurities. Although some elements in alloys might be impurity elements, in other alloys they can be primary elements [4].

- Primary elements: Silicon (Si), Magnesium (Mg)
- Secondary elements: Nickel (Ni), Tin (Sn)
- Modifier elements: Titanium (Ti), Boron (B), Strontium (Sr)
- Impurity elements: Iron (Fe)

2.2.1 Copper

Copper improves tensile strength, fatigue strength and hardness when it combines with aluminium. It decreases ductility and promotes solution heat treatment. Generally it is used in range of 2-10%. Copper also reduces castability and increases hot tear resistance.

2.2.2 Silicon

Silicon improves casting properties, increases the fluidity and reduces the shrinkage of alloy. Si forms an eutectic at 11.7% of Si, 577°C. It reduces workability and improves resistance to abrasive wear. If Si combined with Mg, it allows for strengthening of the alloy by heat treatment. Also it reduces the hot tearing and anodizing ability.

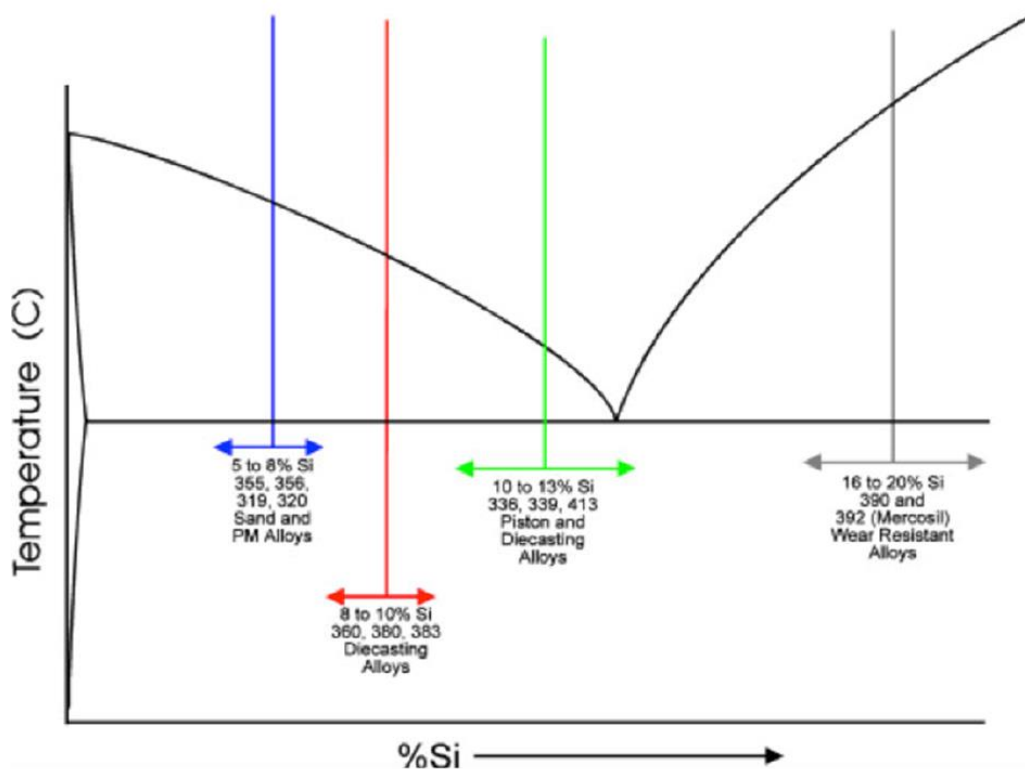


Figure 2.2 : Al-Si phase diagram and aluminium alloys [2].

2.2.3 Magnesium

Magnesium increases strength and hardness when it is added below 0.7% into aluminium. Also it increases corrosion resistance and reduces castability. If Mg is added into Aluminium very small amount, it makes AlSi alloys heat treatable.

Precipitation of Mg_2Si can disperse finely in the matrix and it improves mechanical properties (Figure 2.3).

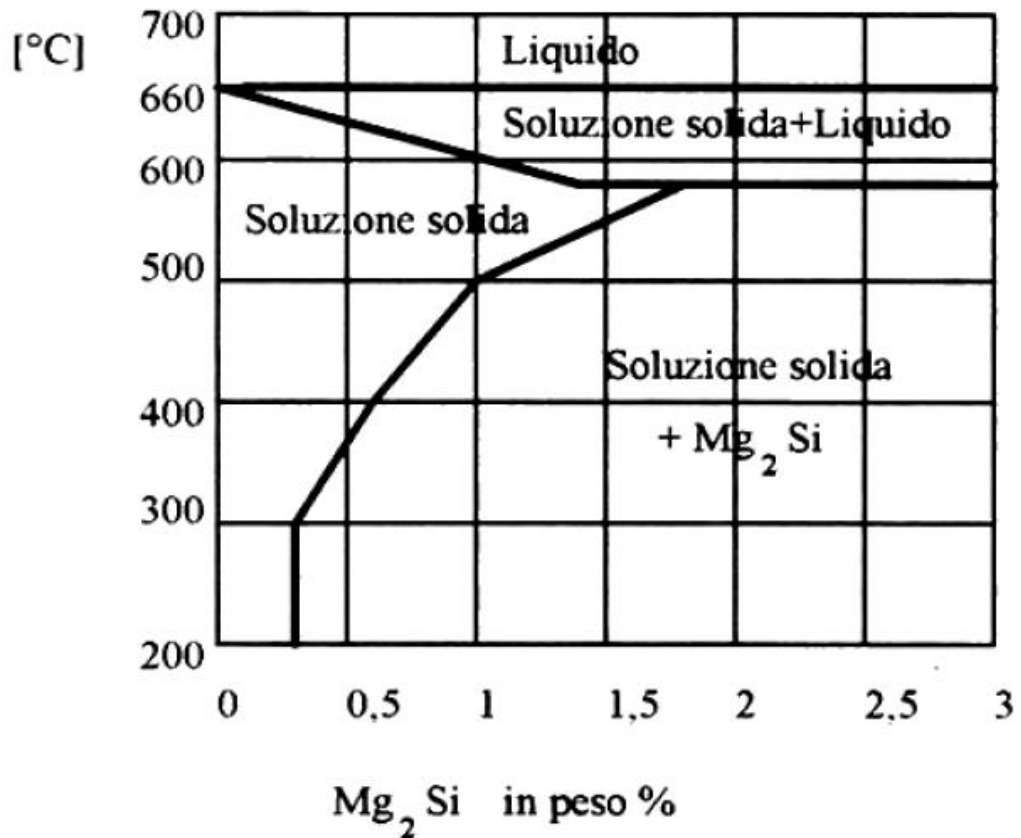


Figure 2.3 : Mg_2Si precipitation in AlSi alloy according to temperature [2].

2.2.4 Strontium

Strontium is used to modify the Al-Si eutectic and effective modification can be achieved at very low addition levels. Casting porosity can be increased in case of adding high amount of Sr.

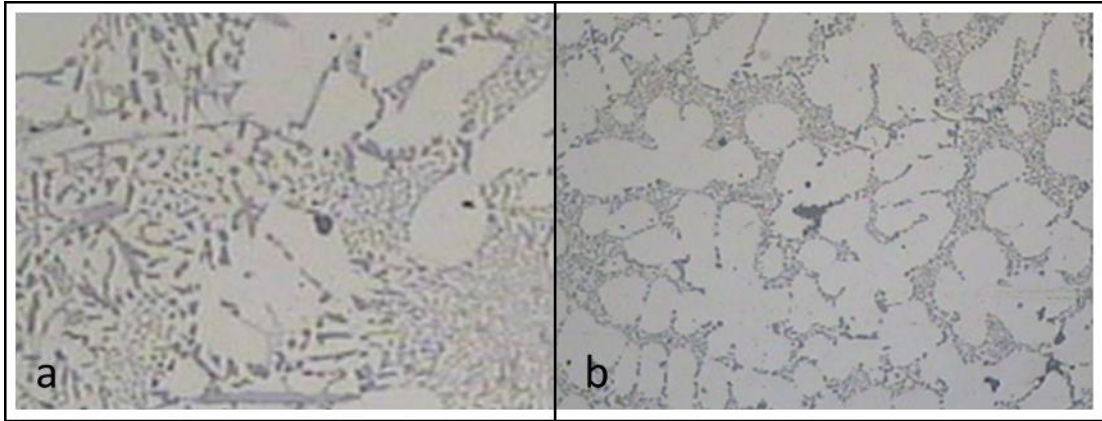


Figure 2.4 : a) not modified microstructure b) modified microstructure after Sr addition [2].

2.2.5 Titanium

It is generally used for grain refinement of aluminum alloy and it is in a combination with a few amounts of Boron. Titanium is not an alloying element and its effectiveness reduces in time. If too much titanium is used it causes sludging of the holding furnace which is very detrimental for casting.

2.2.6 Boron

Boron is added into aluminium from borides such as Al_2B and TiB_2 . These borides acts as nucleation sites with active grain-refinement phases as like $TiAl_3$. B is used as a grain refinement element and it improves conductivity by precipitating V, Ti, and etc.. B can be also used in ratio of 0.005-0.1% alone, but it is more effective when used in combination of Ti. Grain refiner Ti-B alloys are mostly in a 5-to-1 % ratio.

2.2.7 Iron

Iron improves hot tear resistance and decreases the tendency for die sticking or soldering in the casting. Too high iron content forms needles and plates and reduces the strength of the material (Figure 2.5).

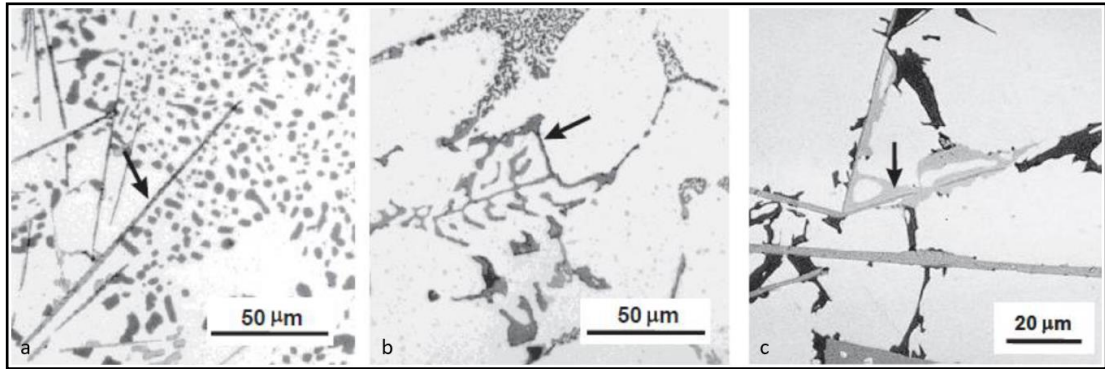


Figure 2.5 : Iron content in AlSi alloys a) Needle β - Al_5FeSi b) Chinese script α - $\text{Al}_8\text{Fe}_2\text{Si}$ c) π - $\text{Al}_8\text{FeMg}_3\text{Si}_6$ [2].

2.3 Low Pressure Die Casting of A356 Alloy Wheels

In automotive industry, Al-Si alloys usage allows the production of light wheels with complex shapes. Low-pressure die castings (LPDC) have the advantage of casting more quality parts with low porosity. It allows a higher production scale than gravity die casting (GDC) processes. Additionally, the mechanical properties of the alloys such as A356 that can be developed by grain refinement during casting. Grain refiners provides finer grains and increase the mechanical and physical properties of the casted products [7].

Casted with A356 alloy wheels are produced from form of ingots. The ingots can be melted in kind of furnaces at $750 \pm 5^\circ\text{C}$. After melting process, degassing process with nitrogen and addition Sr-containing master alloy applied on the molten metal. AlTi_5B_1 rods are used for grain refinement and also they are added to the melt [8].

For melting aluminium below furnaces are generally used:

- Reverberatory furnaces (also called direct contact furnaces)
- Crucible furnaces
 - Bail-out
 - Tilting
- Electric furnaces
 - Resistance
 - Induction

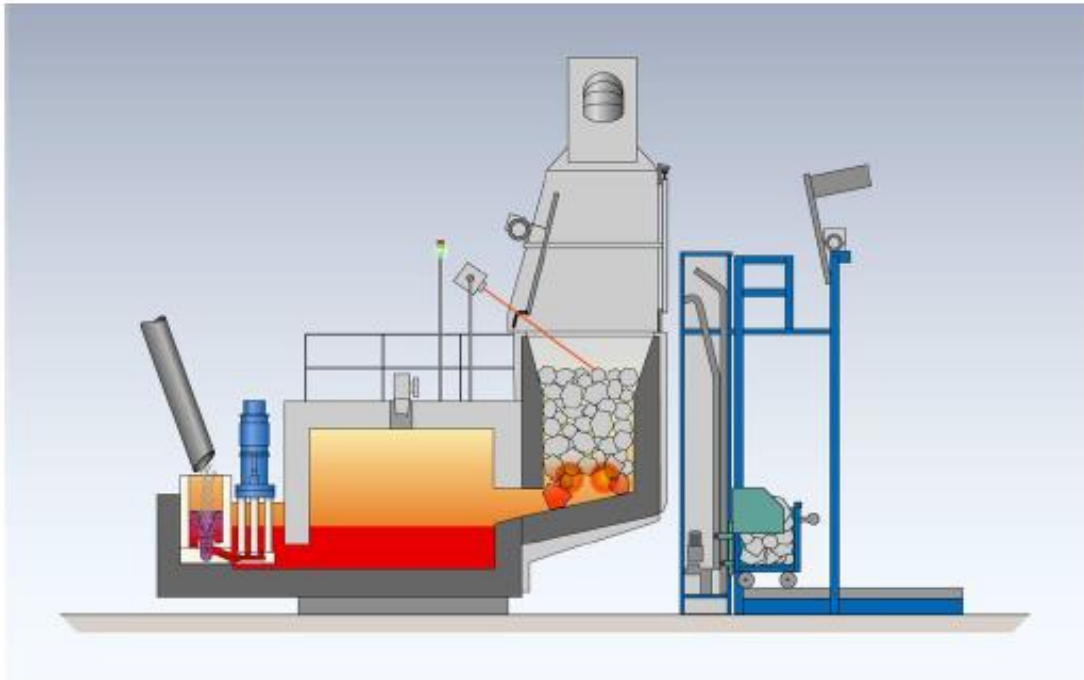


Figure 2.6 : Schematic drawing of reverberatory furnace [6].

After melting ingots and adding alloying elements, deoxidizing and degassing process should be applied to melt. The purpose of these processes are cleaning oxides from the melt and decreasing the hydrogen content.

Rotary degassing equipments have submerging an impeller. Inert gas is injected through the shaft of the impeller during rotation, as shown schematically in Figure 2.6. Degassing process variables are the gases (inert or reactive), impeller turning velocity, gas flow ratio, degassing duration and molten metal temperature. In this process, the rotational speed of the impeller cuts through the gas bubbles while they are passing through the holes which causes a better bubble distribution in the molten metal. Gas bubbles take hydrogen from the molten metal because of the partial pressure difference. Bifilm content increases with gas bubbles ratio in molten metal. Degassing process becomes more efficient whit increasing bubble size [10].

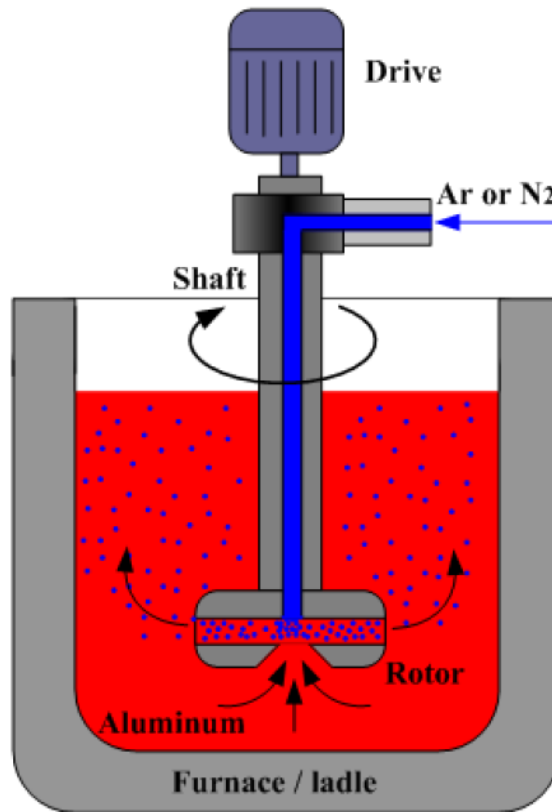


Figure 2.7 : Schematic drawing of reverberatory furnace [9].

After degassing process, melt is poured into transportation crucible and then directly transported to LPDC units. The basic expression of the LPDC is filling the melt into the mold opposite to gravity by pressure, vacuum or electromagnetic pumps. The parts that produced with this method have better mechanical properties than the parts are casted by gravitational force. Casting should be performed very special and under control and these cause to a good ability to cast parts that have very thin sections. Liquid metal can be filled into the mold in three different ways. Previously melt was transported by piston into stable mould. Then the method was upgraded and melt transportation have started to perform by gas pressure. In this method, mold is stayed in isolated mechanism that also includes liquid metal (Figure 2.7). There is a pipe (feeder) below the mold that helps the liquid metal in the mold by gas pressure. Gas pressure is applied on the surface of liquid metal. This is the most common method for wheel casting industry. Convenience to automation systems, low mold cost and ease of application for metal temperature makes LPDC (Figure 2.8) systems more advantageous than traditional casting methods. Although LPDC systems give the casted parts high mechanical properties, some casting defects also can be occurred

during filling the mold by gas pressure [11]. These defects will be explained in next section.

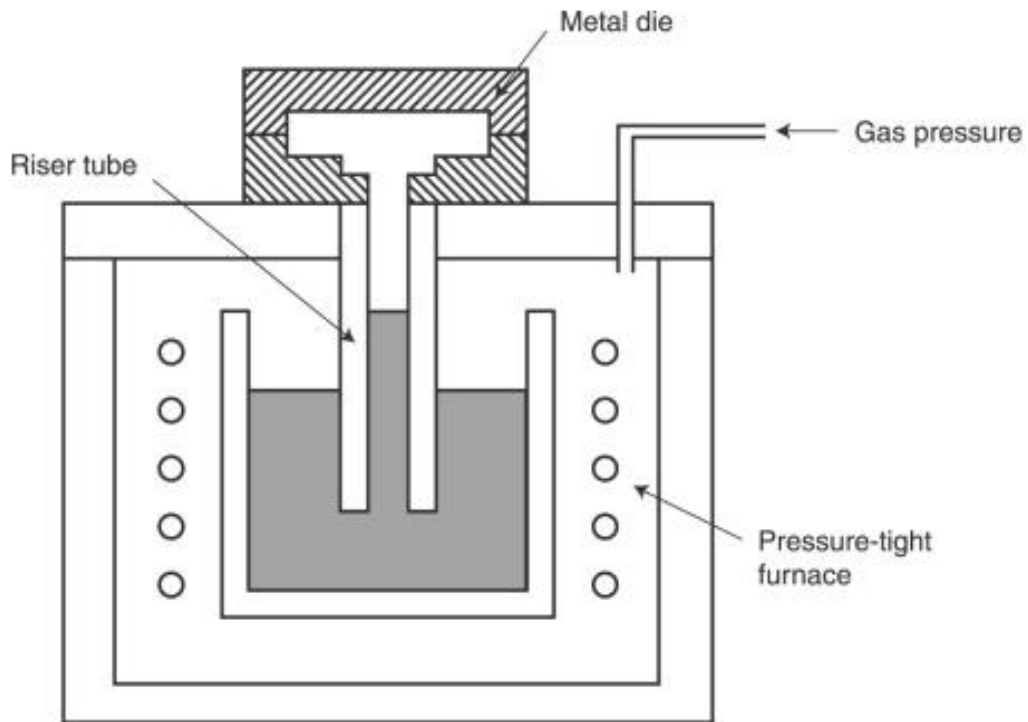


Figure 2.8 : Schematic drawing of LPDC system [12].

2.4 Casting Defects During A356 Wheel Production

Casting defects can be divided firstly in two categories:

- Chronic defects: These are long standing defects that are due to a repetitive condition in the process process should require a modification to eliminate these defects for example changes in the process parameters or mold design.
- Sporadic defects: These defects happen randomly and that can be harder to detect and modify.

Casting defects can occur due to alloy or process itself.

2.4.1 Defects due to alloy

Alloy based defects can be occurred according to;

- Use of not proper alloy, out of range chemical composition
- Presence of impurities: Fe, Pb...

- Improper storage of the alloys such as humidity, oil...
- High amount of chips and flashes in the melt
- Wet and dirty charge

2.4.2 Defects due to melting

If the molten metal temperature is too high it can;

- Increases the Hydrogen absorption
- Increases the risk of oxide formation (even corundum) (Figure 2.9)
- Reduces the life of the refractory wall
- Reduces the life of ladle
- Increases the Fe dissolution

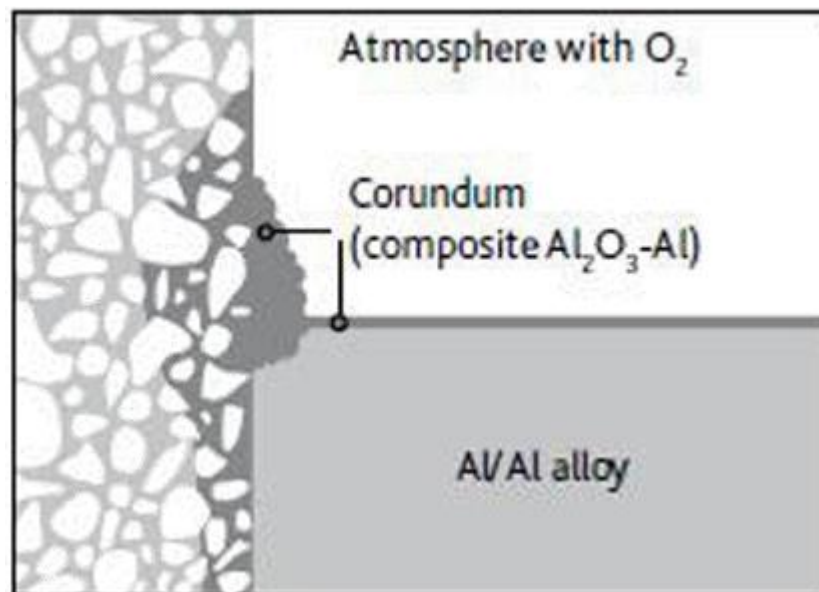


Figure 2.9 : Corundum formation [13].

Addition to these defects, inclusions can be also occurred during melting process due to absorption of oxygen, dirty charge, consumed refractory walls of furnaces and crucibles and pouring phases. Some inclusions are given in Table 2.4.

Table 2.4 : Inclusion types and root causes

Inclusion Type		Origin
Carbides	Al_4C_3	Electrolysis cells, etc.
Boron Carbides	Al_4B_4C	Treatment with B
Titanium Borides	TiB_2	Use of nucleants agent
Graphite	C	Degassing rotors
Chlorides	NaCl, KCl, $MgCl_2$	Fluxes
α -alumina	$\alpha-Al_2O_3$	Oxidation at high temperature
γ -alumina	$\Gamma-Al_2O_3$	During Pouring and transportation
Mg oxide	MgO	High Mg% alloys
Spinel	$MgOAl_2O_3$	Medium/low Mg% alloys

2.4.3 Defects due to casting

There are other defects due to filling conditions (fluid-dynamics), to the improper mold design, to the wrong operative parameters or to the solidification (thermally induced).

They can be classified as follows:

- Gas porosity
- Blister
- Shrinkage porosity
- Heat sink
- Hot tearing
- Cracks
- Oxides (during filling)
- Undesired structure
- Cold flows or cold joints

- Distortions
- Soldering
- Cold shots
- Incomplete casting
- Flashes
- Leakage

Although leakage defect can be defined as a casting defect, it is actually cause of one or several casting defects. Main causes are oxides and porosities. For understanding leakage defect, these there defects should be determined firstly.

2.4.3.1 Oxides (Bifilm)

Nonmetallic inclusions can be occurred the reaction between Al and air. The free surface of the liquid vein is in contact with air inside the mold (Figure 2.10). Because of this situation liquid metal can be easily oxidized. The oxides formed during filling are called “young” and look like very thin film. Additionally oxides can be developed during melting process or during transportation from furnace to crucible from the thickening of already existing oxides. These kind of oxides called as “old” oxides [14].

Excessive turbulence during mold filling can result in the entrainment of portions of this dangerous film. Oxide films can create inside stress and they can cause to fatigue crack initiation.

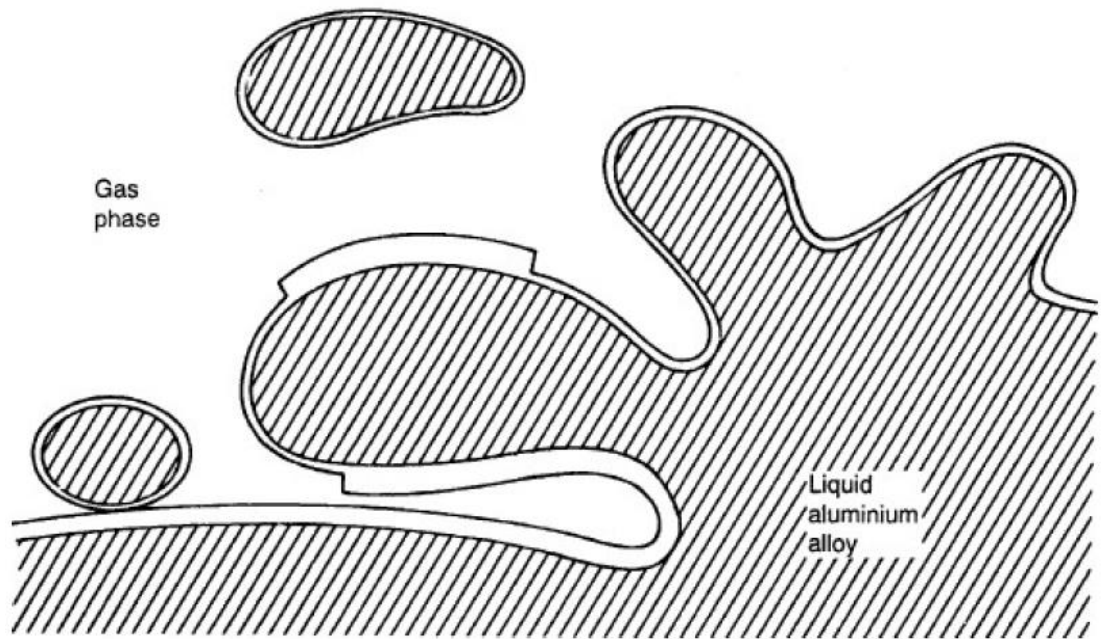


Figure 2.10 : Formation of oxide films [13].

2.4.3.2 Porosity

During formation of porosity defects, bifilms can be accepted as a initiator. Addition to bifilms, hydrogen and air are sidekick for porosity [15].

It can be divided two as:

- Gas porosity
- Shrinkage porosity

Gas porosity can be formed by hydrogen content of molten metal and air entrapment during mold filling. Also these can be defined as “hydrogen porosity” and “air porosity”. Although hydrogen porosity is almost spherical, air porosity can be appeared as spherical, oval and tear drop shaped.

Shrinkage porosity occurs in areas where there is not enough feeding of molten metal to center zone. The shrinkage is generally related with transformation between solid and liquid. All these types of porosity are given in below (Figure 2.11).

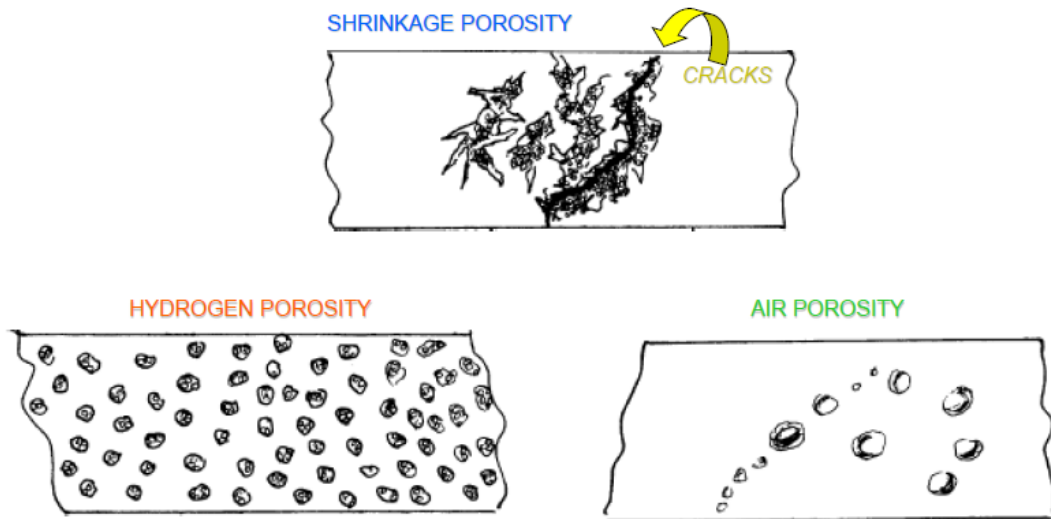


Figure 2.11 : Shapes of shrinkage, hydrogen and air porosity [13].

2.4.3.3 Leakage defetcts

Oxide films and porosity absence can create leakage problem in every type of casting. Especially in wheel production, it is one the most unwanted defects (Figure 2.12). It is located on rim area of the wheel and cannot be detected during casting process. After casting is completed, wheels are machined. At the end of machining process all wheels are controlled in dry/wet leak test machined. If there is a small leakage on rim surface, wheel is scrapped.

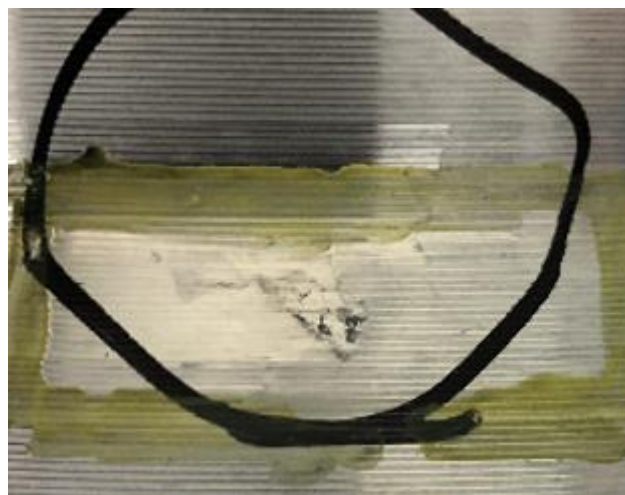


Figure 2.12 : Leakage defect on rim surface

3. COLD SPRAY

Cold Spray has different names such as: Cold Gas Dynamic Spraying, Kinetic Spraying, High Velocity Particle Consolidation (HVPC), High Velocity Powder Deposition and Supersonic Particle/Powder Deposition (SPD). In a cold spray process, there is a high speed gas jet that changes between 300-1200 m/s, formed using a deLaval or similar nozzles, is used to accelerate powder particles (1 to 50 μm) and spray them onto a substrate, located approximately 25 mm from the exit of the nozzle where they impact and form a coating. Instead of high temperature there is a kinetic energy of the particles that helps these particles to plastically deform on impact and form splats, which bond together to produce coatings and thereby avoids or minimizes many deleterious shortcomings of traditional thermal spray methods such as high-temperature oxidation, evaporation, melting, crystallization, residual stresses, and gas release. Powder particles are accelerated by the supersonic gas jet at a temperature that is always lower than the melting point of the material. This results a solid state coating formation from particles and there is no melting and solidification process that is experienced by the powders like in traditional thermal spray process [16; 17].

3.1 History of Cold Spray

The cold spray process was originally invented in the 1980s by Alkhimov et al. They patented in 1986 the first two cold spray patents that were issued in 1991 in the Soviet Union. The first patent claims a coating method for accelerated powder particles (650-1200 m/s) to a substrate by unheated gas steam. The second patent claims a device that is using previous method with a mixing chamber, intermediate nozzle, a feeder and supersonic rectangular nozzle (Figure 3.1). They succeeded to deposit several metal powders on different materials [18; 19].

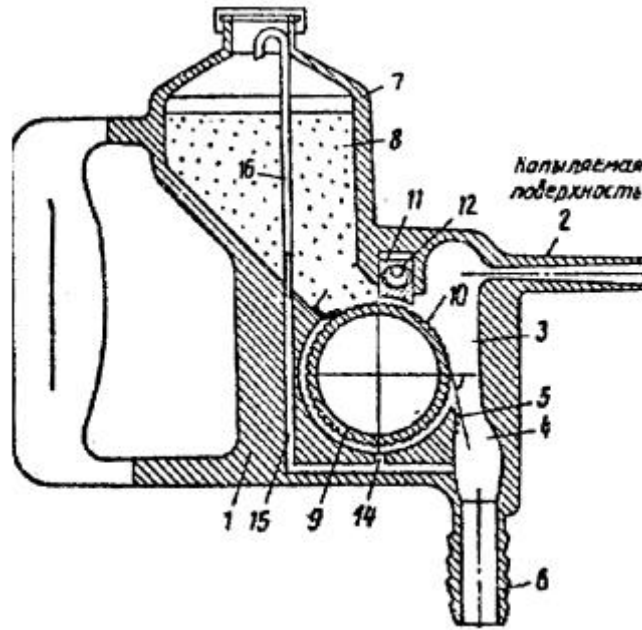


Figure 3.1 : First patented cold spray device [19].

After successfully completed feasibility studies, preheated gas chamber was investigated and patented. In 1994 U.S. patent and in 1995 European patent was issued by Anatoly Payrin. It is mentioned in these patents as high pressure cold spray method. Kashirin et al. modified a device for the injection of powder particles In 1996. This device provides feeding the powder material from the feeder-dispenser through separate line into the diverging part of the nozzle. After this invention Nikitin et al. patented the first portable cold spray apparatus in 2004 (Figure 3.2). This device contains a pistol type body with a DeLaval nozzle, powder mixing chamber, powder and gas feeding pipes [19].

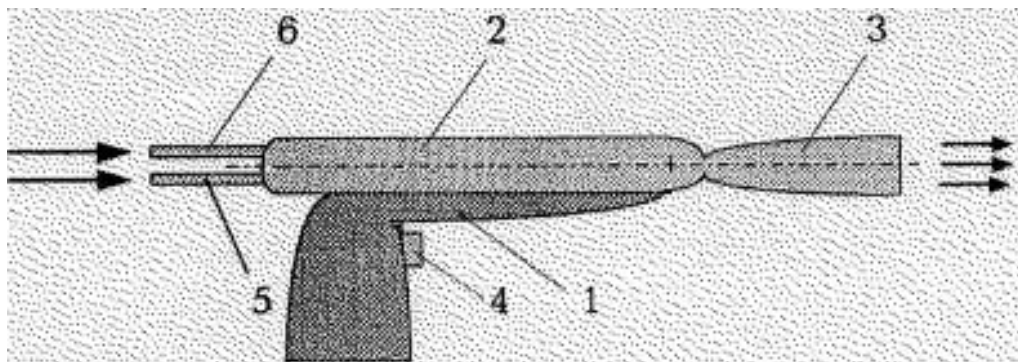


Figure 3.2 : First portable cold spray gun [19].

3.2 Areas of Usage

Cold Spray method is gaining in popularity day by day. Reduction in material input, elimination of mold cost, reduction in rework, reduction in finishing and low material utilization (deposition efficiency 60-95 %) are important advantages that are provided by cold spray applications [20]. General applications that cold spray can be used is listed below.

- Repairing corrosion damage (Figure 3.3)
- Recovering mis-machined parts
- Improving wear resistance (CrC-NiCr, WC-Co, WCu coatings)
- Restoring worn/damaged features (Figure 3.4)
- Preventing corrosion damage
- Surface build up (Figure 3.5)
- Providing conductive properties
- Improving dielectric properties
- Thermal management coatings
- Enhancing surface conductivity
- Biomedical – prostheses with improved wear
- Die casting- extending die life
- Printing – copper coating on rollers [20; 21].

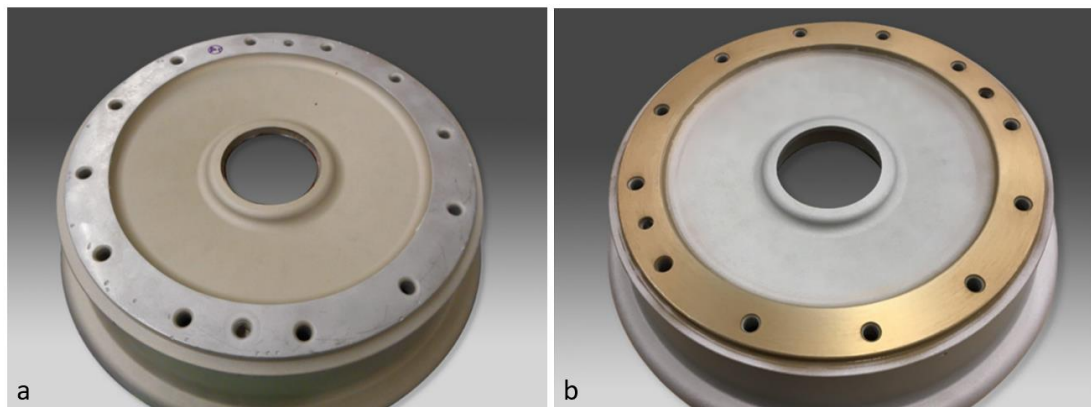


Figure 3.3 : a) Corroded T-6 Aircraft Wheel b) After Cold Sprayed T-6 Aircraft Wheel [21].

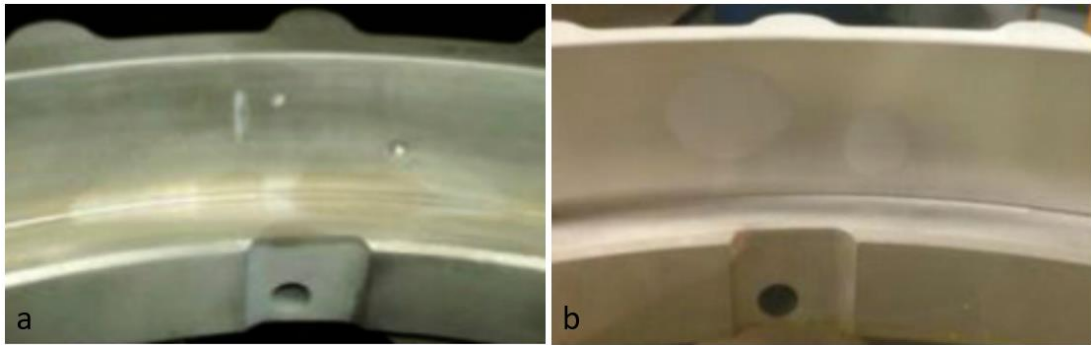


Figure 3.4 : a) Magnesium Casting Defect b) Cold Sprayed Repair Casting [21].

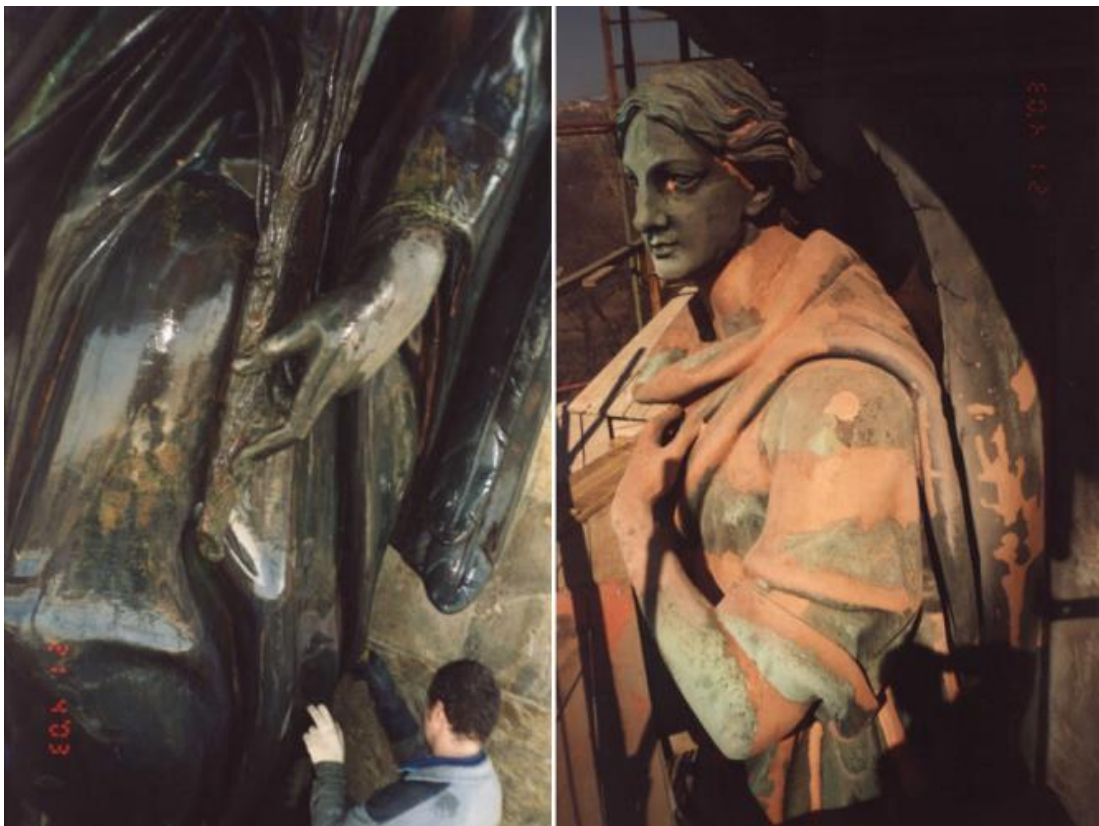


Figure 3.5 : Restoration of an old sculpture by cold spray method [22].

3.3 Main Components and Basic Process Description

Metal powders are utilized as a deposit by means of ballistic impacting by means of impacting on a substrate in cold spray process. 5-100 μm particle sized metal powders are accelerated by injection into a high-velocity stream of gas. The expansion of a pressurized, preheated gas through a nozzle creates high velocity gas stream. The separate gas stream carries the powder particles, and then particles are injected into the nozzle either at the nozzle entrance or at a lower pressure point downstream of the

entrance. The main nozzle gas flow accelerated the particles and then are impacted on a substrate after exiting the nozzle. If the particles are above a critical velocity, they will deform and bond in a dense layer on substrate. Particles continue to impact the substrate and form bonds with the previously deposited material. It will resulting in a uniform deposition with very little porosity and high bond strength [23]. All stages of coating formation is given in Figure 3.6.

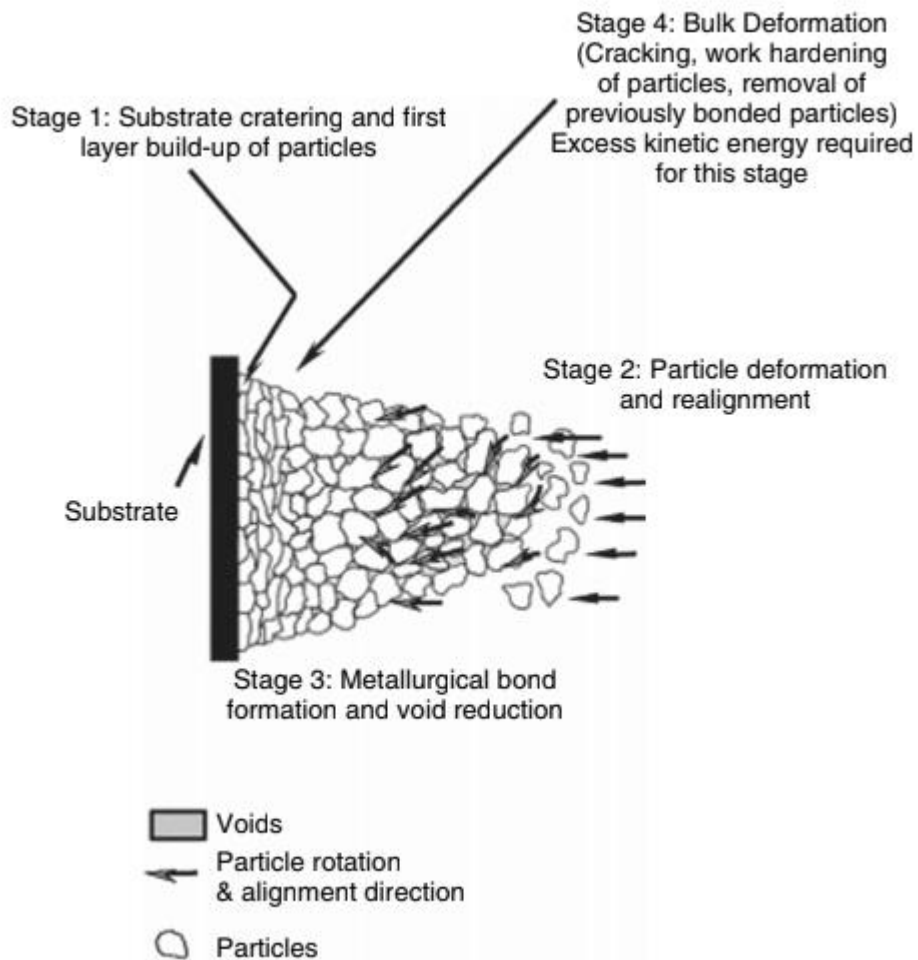


Figure 3.6 : Cold spray process formation levels [25].

The main components of cold spray are:

- Powder feeder (powders used are in the range of 1 to 50 μm in diameter)
- Source of a compressed gas
- Gas heater to preheat the gas, to compensate for the cooling due to rapid expansion in nozzle
- Supersonic nozzle (Delaval nozzle)

- Spraying chamber with a motion system
- System for monitoring and controlling spray parameters (to measure and control the gas temperature and pressure) [24].

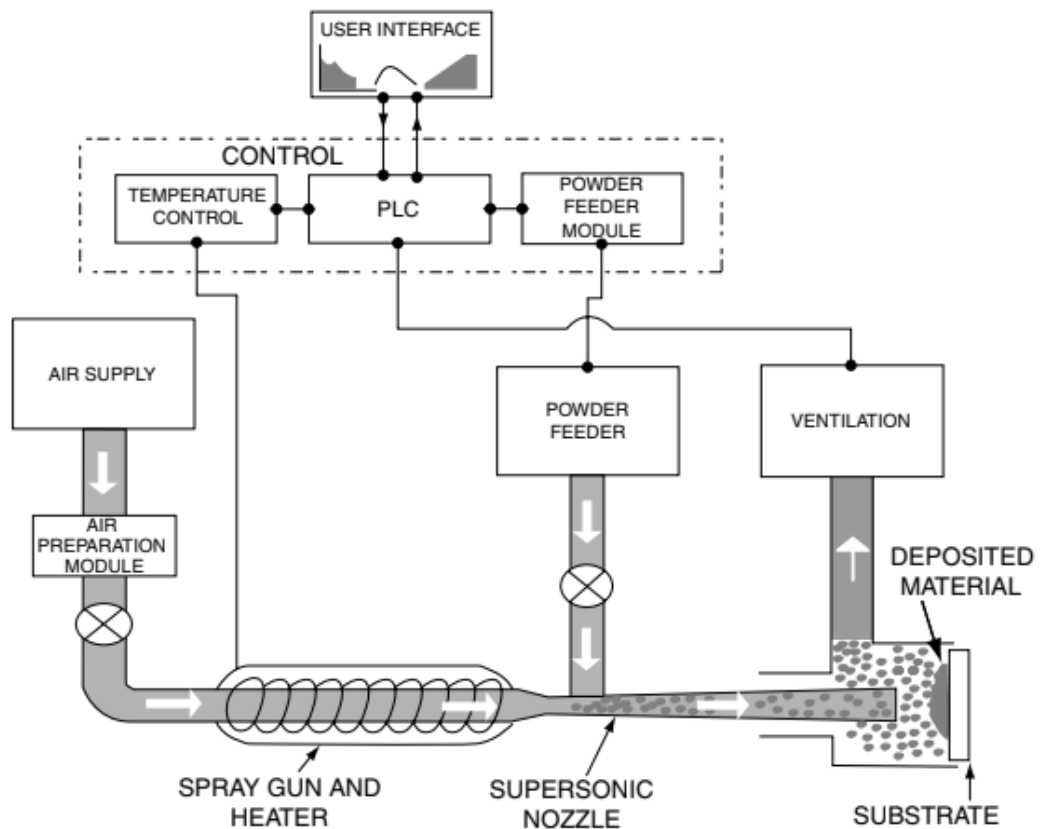


Figure 3.7 : Schematic diagram of the cold spray SST Centerline system [23].

In cold spray process, there are four different gasses are generally used. These are:

- Helium
- Nitrogen
- Mixture of He and N
- Dry air (79%N -21%O)

Helium is mostly known as the most efficient gas that is used in cold spray processes. It increases the deposition efficiency and decreases the oxidation. But He costs much more than the other gasses that can be used.

One of the most important parameters in cold spraying is particle velocity (V_p). It determines a deposition of a particle or erosion of a substrate during spraying of

particles. Materials have a minimum particle velocity commonly known as critical velocity (V_c) which must be achieved for deposition on a sprayed substrate instead of erosion. If $V_p < V_c$ particles reflect from the surface. In $V_p = V_c$ condition solid particle erosion occurs on the surface. The deposition can be occurred just in $V_p > V_c$ condition. The critical particle velocity of the metals are such as: 560–580, 620–640, 620–640 and 680–700 m/s, for Cu, Fe, Ni and Al respectively [24].

The second important parameter of cold spraying is “Standoff Distance” that is defined as the distance between nozzle outlet and the surface (Figure 3.8). While the standoff distance increases from zero, particle impact velocity and deposition efficiency increase till an optimum operating point. This situation has been experimentally confirmed in many studies especially aluminum and copper deposits. Mostly used standoff distance is 10-40 mm for manufacturing [26].

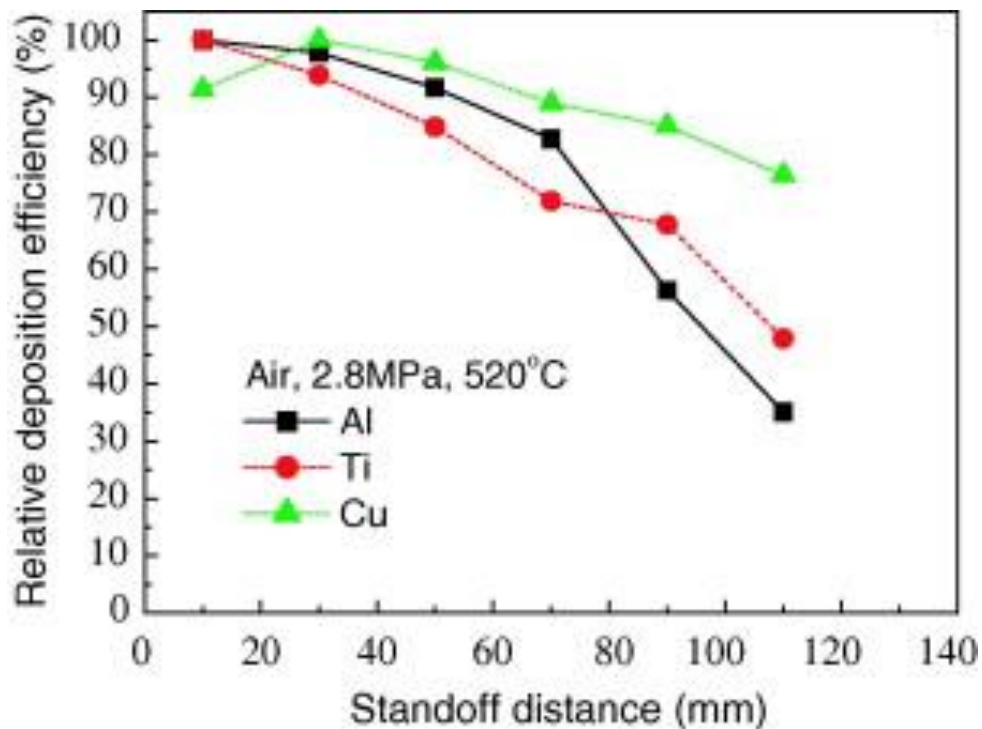


Figure 3.8 : Corelation between Standoff distance and deposition efficiency [26].
 The third important parameter is the gas temperature. Increasing gas temperature decreases porosity volume and porosity sizes. Particles deforms easily with high gas temperature and it decreases empty spaces. This situation also increases deposition efficiency [27].

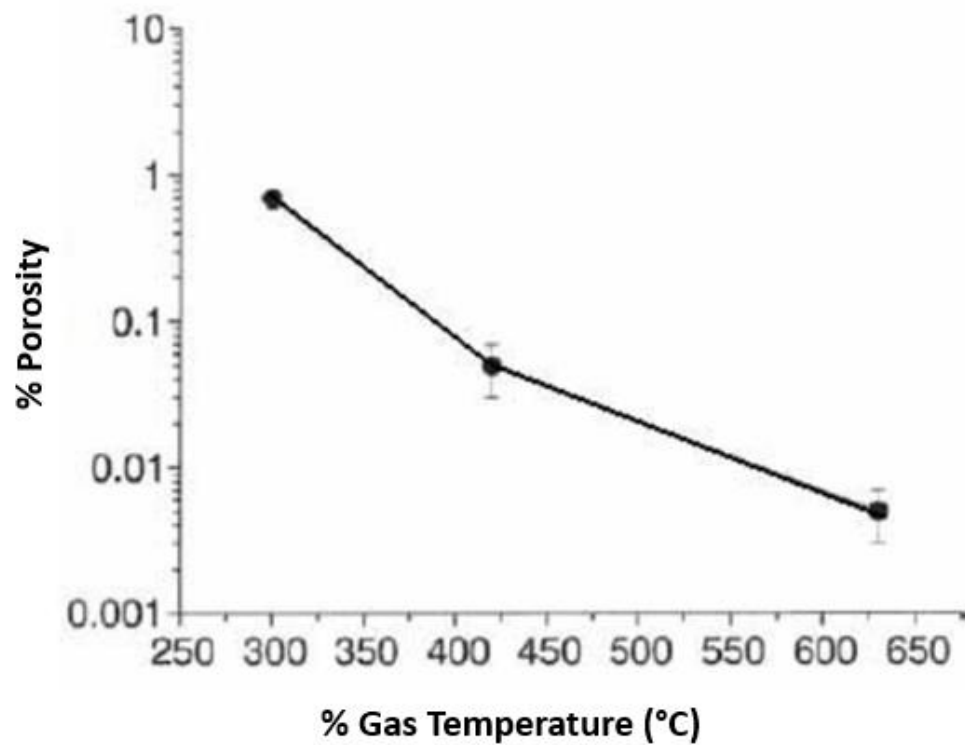


Figure 3.9 : Corelation between Gas temperature and % porosity in Cu based coating [27].

There are two different systems of cold spray process. These are:

- High Pressure Cold Spray
- Low pressure Cold Spray

Main differences between two systems are gas types, gas temperature, gas pressure, particle size distribution. All parameters and systems will be explained in next section.

3.4 High Pressure Cold Spray

High-pressure system in which the main gas stream and the powder stream are both introduced into the inlet chamber of the nozzle it is illustrated in Figure 3.10. HPCS requires that the powder feeder be capable of high gas pressure and is most often used in stationary cold spray systems (Figure 3.11). HPCS systems uses higher pressure gases and have a gas compressor. System uses a low molecular weight gas, such as helium, as the accelerating gas when particles must be brought to critical velocity [23].

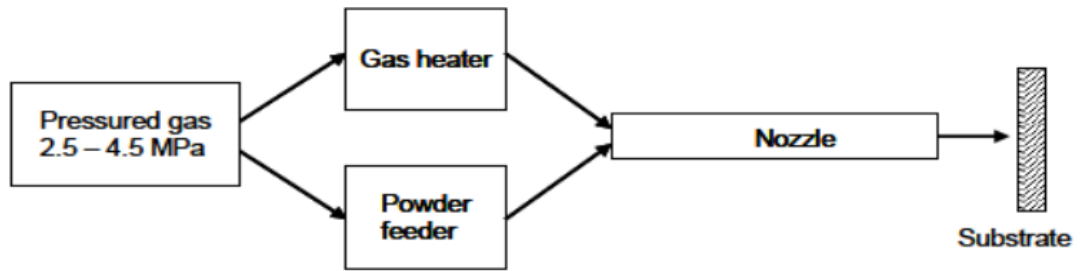


Figure 3.10 : Schematic diagram of HPCS system [23].



Figure 3.11 : Image of commercial stationary HPCS system [27].

In high pressure cold spray (HPCS) particles are injected prior to the spray nozzle throat from a high pressure gas supply. In HPCS, the gas (helium or nitrogen) at high pressure (25-30 bar) is heated (up to 1000°C) for its better aerodynamic properties (not to increase particle temperature) and then injected through DeLaval nozzle. The solid particles are accelerated to 600 - 1200 m/s and impact the substrate with enough kinetic energy to induce mechanical and/or metallurgical bonding. The deposition efficiency in HPSC system is very high (up to %90) [28].

3.5 Low Pressure Cold Spray

Powder stream is injected into the nozzle at a point where the gas has expanded to low pressure, it is illustrated in Figure 3.12. Atmospheric pressure air that is coming by the lower pressure nozzle injection point, is used for powder transport from the feeder. For this reason LPCS system does not require a pressurized feeder and it is used in portable

cold spray systems. The low-pressure system generally uses readily available compressed air, but it can be used Nitrogen if it is needed.

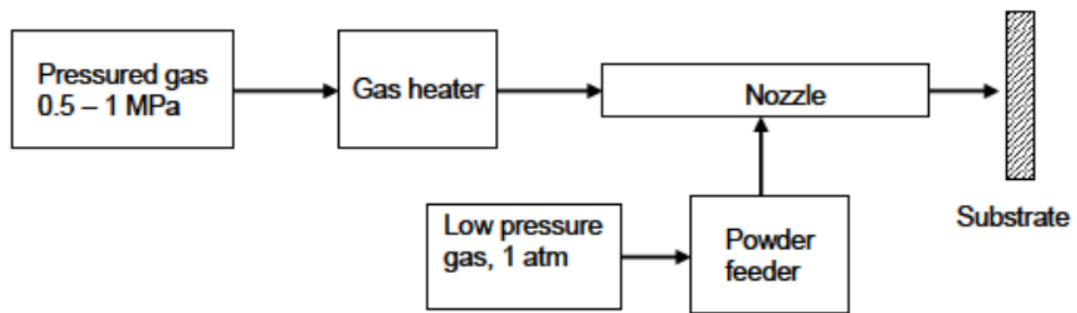


Figure 3.12 : Schematic diagram of LPCS system [23].

In LPCS system powders are injected in the diverging section of the spray nozzle from a low pressure gas supply. LPCS systems are generally smaller and portable and in these systems, the gas is usually dry air or nitrogen, at relatively low pressure (5-10 bar) and heated (up to 550°C) for its better aerodynamic properties and injected through a DeLaval nozzle. The heated gas is accelerated to 300 - 600 m/s. Modern LPCS equipment is designed as portable or mobile system for both manual and robotic operation. Commercial DYMET and SST (in North America) systems are using for many applications. Compact spraying gun, control unit and open powder feeders are the main components of the system and these are given in Figure 3.13 [18, 24].



Figure 3.13 : Commercial LPCS equipment and automated spraying gun system [22].

Materials such as Zn, Al and Cu are ideal for LPCS systems because they have relatively low melting point and low mechanical strength. They also have a low yield strength and show significant softening at elevated temperatures. Low process temperatures are needed for dense coatings with these materials. The deposition of Al

is sometimes is more difficult than other soft materials such as Zn and Cu. This is because of its high heat capacity that makes it more difficult to deposit, although Al has low melting point and low yield strength [28].

Because of their low density, high tensile strength, good formability and corrosion resistance aluminium and its alloys are generally used in aircraft, marine and automotive components. For an example, the helicopter mast support is an component that is manufactured using aluminium alloys. The typical damage that decreases the service life of it, is the corrosion pitting on the snap ring groove surface. When this damage is occurred, the mast support must be repaired or replaced. Instead of scrapping the component, LPCS can be used to repair the damage. LPCM has been also applied to the repair of corroded internal bore surface of navy aluminium alloy valve actuator. Additionally corroded oil pump housings of Caterpillar-3116 and Caterpillar-3126 engines with aluminium alloy are repaired by cold spray methods. It was reported that more than 30 corroded pump housings were restored via cold spray from 2012 to 2013 in Moscow. There are no failure report after the components have returned to service [26].

Winnicki et al. has investigated gas pressure and temperature effect on Al+Al₂O₃ deposition by LPCS. In their study commercially available spherical powder powder (Al + 60wt.-% Al₂O₃, -50+10 µm) is embedded on substrate by low-pressure cold spray unit, DYMET 413. Before spraying, the substrate subjected to grit blasting using alumina with particle granulation -350 µm as abrasive material at the pressure of 0.6 MPa. All trials are carried out with compressed air and Standoff Distance is chosen as 20 mm. Powder mass flow rate is 40 g/min and nozzle diameter is 5 mm. they have found that increase of temperature is of much higher effect on the coating thickness than that of pressure increase. Higher pressure allows the particles to exceed the critical velocity and to deposit them on substrate. Temperature affects in two ways. It makes high deposition efficiency and more dense coating [29].

Also there is an important factor that affects the adhesion of the coating. In several studies that is mentioned that amount of added ceramic powder increases the adhesion. Ceramic powders can removes oxides from the surface and by tamping effect makes the metal powder work hardening. It significantly decreases the porosity of the coating.

Winnicki et al. has also investigated the bond strength of Al+Al₂O₃ deposition by LPCS. Commercially available powder of aluminium K-10-01 (Al + 60 wt.% Al₂O₃) is sprayed using a low-pressure cold spraying device, DYMET 413. Before spraying, the substrate subjected to grit blasting using alumina with particle granulation -350 µm as abrasive material at the pressure of 0.6 MPa. Standoff distance is chosen as 10-20 mm. They mentioned that the structure is similar in both cases and consists of aluminium particles, alumina particles, aluminium oxide and pores. The presence of alumina provides high density of the coating by work hardening decreases amount of pores [30].

4. EXPERIMENTS

4.1 Material and Method

Commercial low pressure cold spray equipment Dymet 423 (Figure 4.1) is chosen for coating the wheels which have leakage defects. Dymet 423 is a portable, 18 kg weighted device that can easily deposit aluminium, copper, zinc, lead and nickel metal powders on substrates. It has two separated powder feeder that provides easy switch to different powder during coating process. In some cases, before deposition metal powders to substrate the surface should be cleaned and sand blasted. Sand blasted surfaces are more available for deposition in cold spray process. Because mechanical bonding increases with surface roughness. While one feeder is used for coating material, the other one can be used for abrasive materials such as alumina, quartz, etc....



Figure 4.1 : Dymet 423 LPCS equipment

Dymet 423 is adjustable for feed flow rate and gas temperature. It has 1-10 feed flow rate levels and 1-5 gas temperature levels. Compressed air and Nitrogen can be used

as a carrier gas during coating. It is available for spray metal powders with maximum 6 bar gas pressure.

Commercial metal powder K-00-04-16, K-20-11, SST-A5006 powders were used in Dymet 423. All technical data sheets are given respectively in Appendix A, Appendix B and Appendix C. K-00-04-16 is aluminium oxide ceramic powder and it was used for surface roughness.

Chemical composition of powders were analyzed by Carl Zeiss 300VP Scanning Electron Microscope and EDX equipment with 2000x magnification and 15 kV (Figure 4.2).



Figure 4.2 : Carl Zeiss 300VP SEM

Particle size distribution of powders were analyzed by Malvern Master Sizer 3000 equipment with 1,000 Dispersant Refractive Index, 1,766 Particle Refractive Index and dry dispersion (Figure 4.3).



Figure 4.3 : Malvern Master Sizer 3000

After optimum parameter experiments coatings were investigated for their microstructure and thicknesses under Nikon Eclipse MA 100 microscope with Clemex Image Analyses System (Figure 4.4).



Figure 4.4 : Nikon Eclipse MA 100 with Clemex Image Analyses System

After coating leakage defects rim surface of wheels were investigated by Bosello WRE Thunder 3 X-ray equipments with 85 kV and 5 mA parameters (Figure 4.5).



Figure 4.5 : Bosello WRE Thunder 3 X-Ray System

4.2 Experiments for Optimum Parameter

Before coating leakage defect area, parameter studies were done. To determine optimum parameters, five equal rectangular area separated to 8 equal square areas. Each rectangular areas represent five gas temperature steps that Dymet 423 has and each square areas represent 3-10 powder feeding rate. 1st and 2nd steps of feeding rates are not included in parameter experiments because feeding is very less to determine. All square parts were blasted with K-00-04-16 first then sprayed for 5 seconds with K-20-11. The coated areas are shown in Figure 4.6.

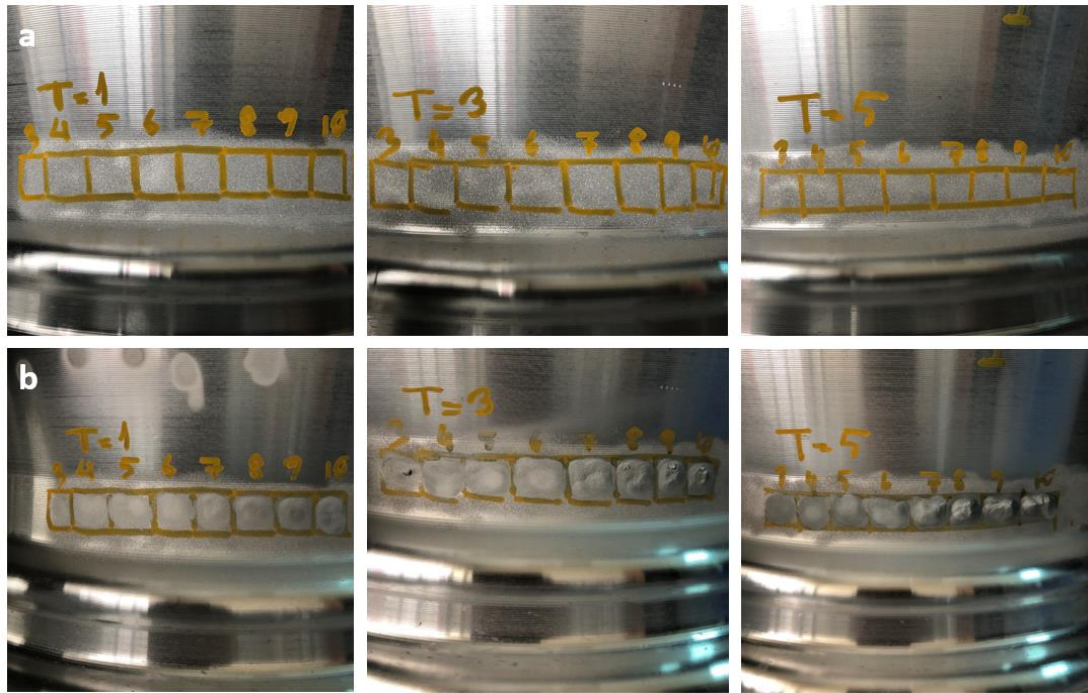


Figure 4.6 : a) Blasted rim surface with K-00-04-16 b) Coated rim surface with K-20-11

After coating process was finished all square areas were cut in the middle with sawing machine. All parts were grinded and polished after cutting and investigated microstructure, porosity level and coating thickness. The coating thicknesses of 40 square parts will be given in Results and Discussion section. After determination of K-20-11 coating parameters, SST-A5006 powder parameters were investigated.

4.3 Experimental Procedure for Leakage Defect Coating

After powder and all coating parameter were determined, experimental procedure of leakage defect coating was planned. 37 pieces of A356 alloy wheels were collected for their different defect levels. The images of rim surfaces which have leakage defect were shown in Figure 4.7.

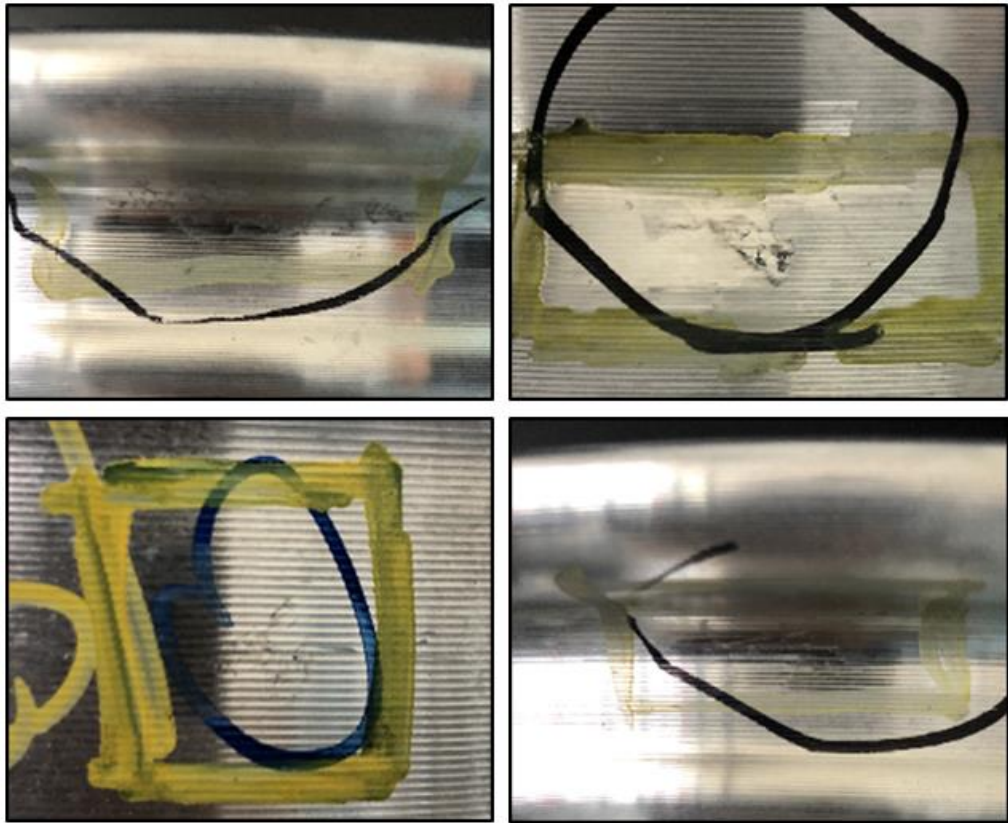


Figure 4.7 : Some examples of leakage defect areas on rim surface

All defected areas were blasted with K-00-04-16 alumina powder as done in parameter experiments section. K-20-11 powder was coated on blasted surface with using 3rd temperature level and 6th feeding rate level of Dymet 423 LPCS equipment. The coated surfaces are given in Figure 4.8. As seen in images, there are crater shaped excessive material on defected areas. After coating process were completed, all excessive materials were grinded for a smooth surface.

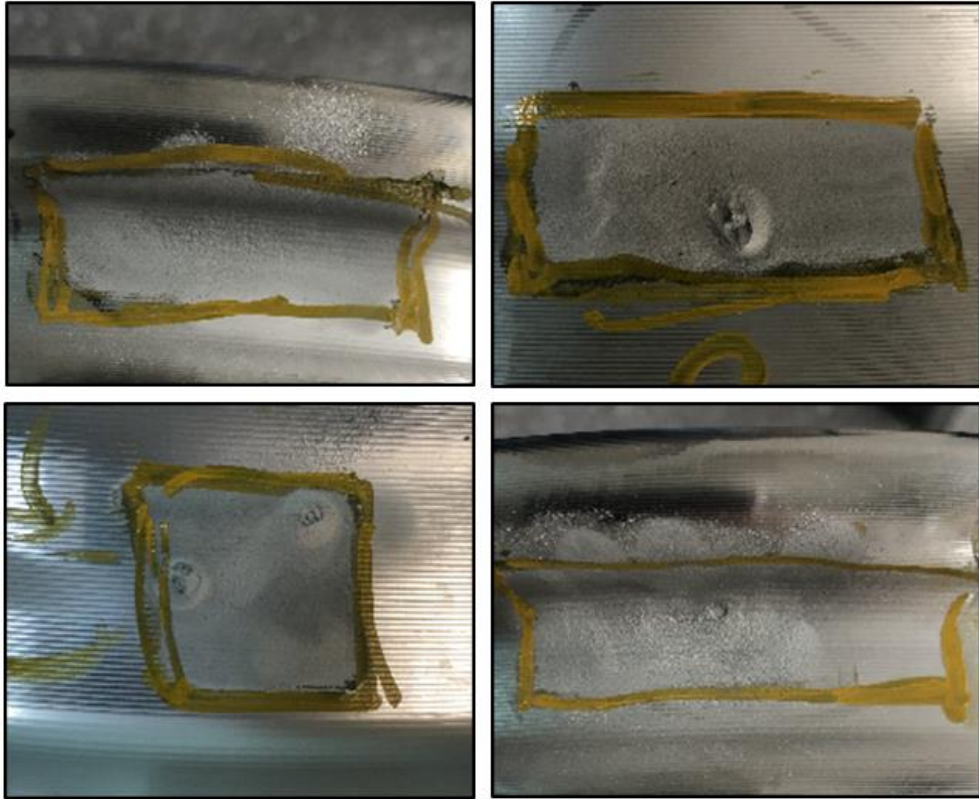


Figure 4.8 : Some examples of coated leakage defect areas on rim surface
Coated and grinded 37 wheels were examined in wet leakage testing machine. In leakage testing methods, wheels were in completely water and by means of high pressure air, leakage areas can be detected by bubbles. Testing equipment and an example of leakage defect is given Figure 4.9.

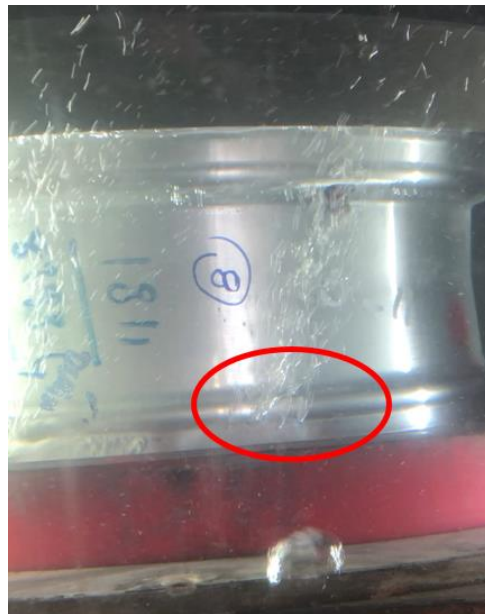


Figure 4.9 : A wheel that has leakage defect

Approved wheels after leakage testing, were controlled in X-ray equipments, mechanical performance tests applied and their microstructure were investigated.

These tests are;

- Hardness Test
- 90° Impact Test
- Radial Fatigue Test

All tests result were compared with customer's specification and they will be given in next section.

5. RESULTS AND DISCUSSIONS

5.1 Powder Characterization and Parameter Experiments Results

Before coating A356 alloy casted wheel, surface was blasted with this powder for better bonding between wheel surface and coating. K-20-11 is a mixture of aluminium oxide (23-27 %), aluminium (33-37 %) and zinc (38-42 %) powders. SEM image is shown in Figure 5.1 and EDS analysis is shown in Table 5.1. K-20-11 is generally used for repair application. As mentioned in previous sections, Al_2O_3 content of this powder decreases porosity and provides better coating. Particle size distribution is 15 - 45 μm and shown in Figure 5.2. This powder is available for spraying by Dymet 423.

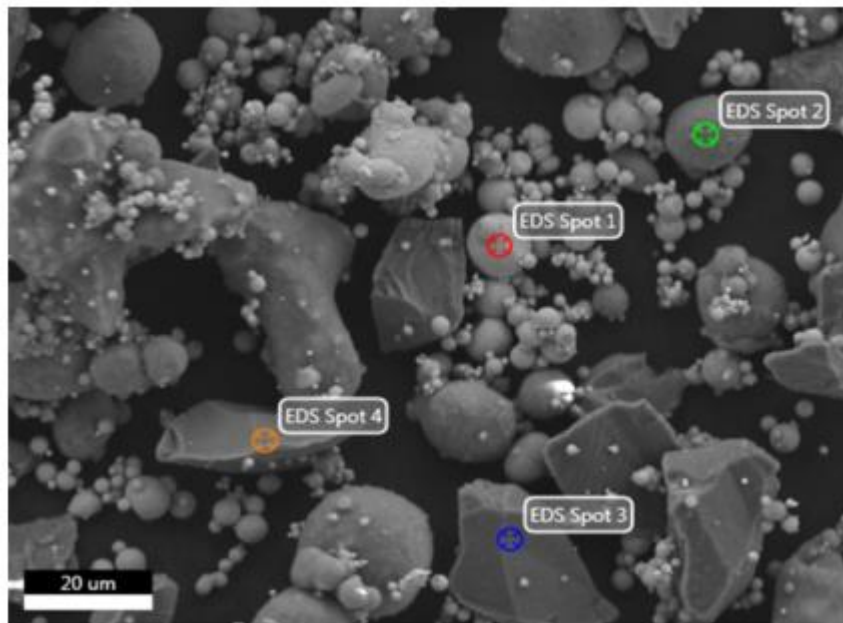


Figure 5.1 : SEM image of K-20-11

Table 5.1 : EDS analysis of K-20-11

	EDS Spot 1	EDS Spot 2	EDS Spot 3	EDS Spot 4
Al (Weight %)	2,04	97,75	49,21	51,33
Zn (Weight %)	96,43	-	-	-
O (Weight %)	1,53	2,25	50,79	48,67

K-20-11 is generally used for repair application. As mentioned in previous sections, Al_2O_3 content of this powder decreases porosity and provides better coating. Particle size distribution is 15 - 45 μm and shown in Figure 5.2. As Winnicki et al. mention in their study shows that 10-50 μm powder distribution is available for Dymet equipments [29].

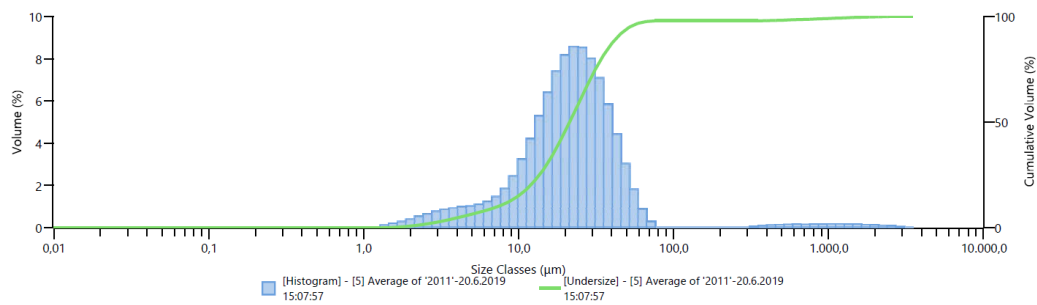


Figure 5.2 Particle size distribution of K-20-11 (Dv (10) 7,31 μm , Dv (50) 21,4 μm Dv (90) 43,3 μm)

After parameter experiments are completed with K-20-11 powder, another commercial powder SST-A5006 will be used. Instead of K-20-11, SST-A5006 powder is alloy powder and chemical composition is very similar to A356 alloy. SEM image is given in Figure 5.3 and EDS analysis is given Table 5.2.

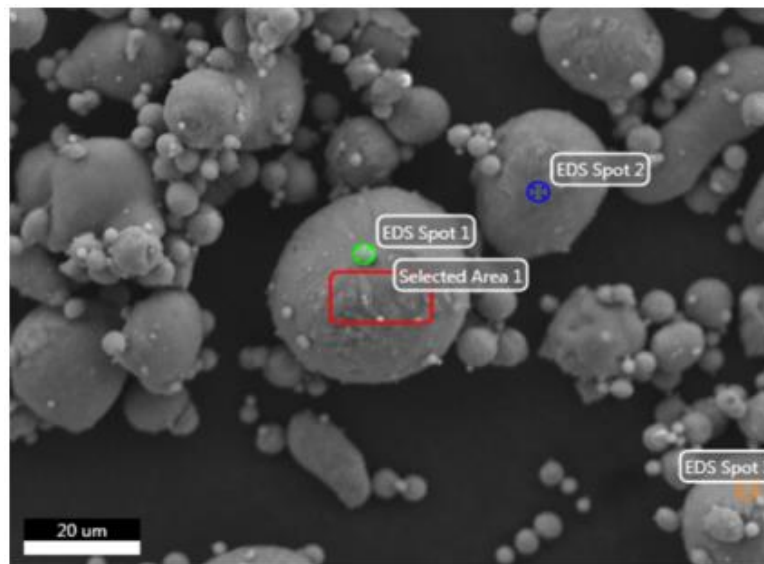


Figure 5.3 : SEM image of SST-A5006

Table 5.2 : EDS analysis of SST-A5006

	S. Area 1	EDS Spot 1	EDS Spot 2
Al (Weight %)	87,04	86,10	82,49
Si (Weight %)	12,96	13,90	17,51

Addition to chemical composition similarity, SST-A5006 powder's particle size distribution is also similar to K-20-11 powder (Figure 5.4). SST-A5006 powder is a little thicker than K-20-11 and not included ceramic powders such as alumina. As mentioned previous sections small amount of alumina or other ceramic powder existence increases deposition efficiency. Although manufacturer of SST-A5006 mentioned that this powder is not suitable for Dymet 423 equipment, same parameter experiments will be done and will be investigated for availability of coating.

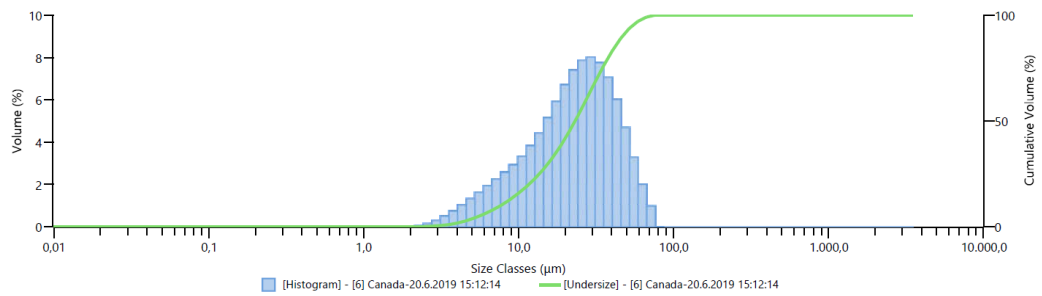


Figure 5.4 : Particle size distribution of SST-A5006 (Dv (10) 7,63 µm, Dv (50) 23,2 µm Dv (90) 46,9 µm)

After parameter experiments, all coating thicknesses were measured (Table 5.3) and optimum temperature step was defined as 3rd level and powder feeding rate was defined as 6th level (Figure 5.5).

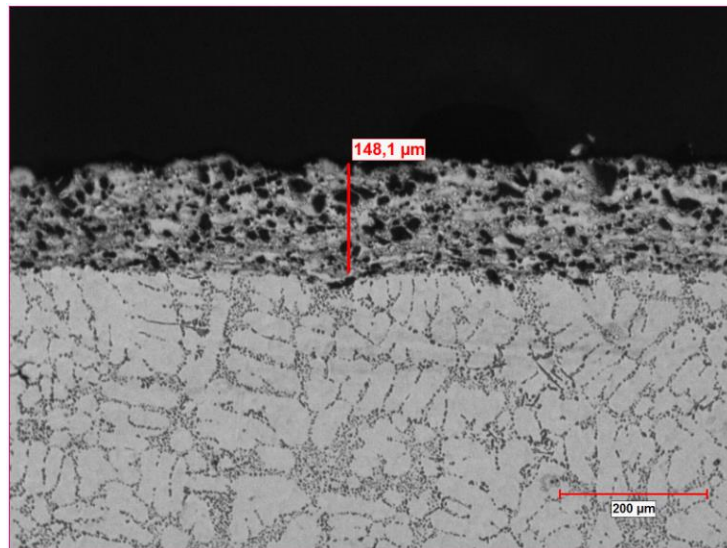


Figure 5.5 : Microstructure under optical microscope of 3rd temperature and 6th feeding rate level (Optimum Condition)

Table 5.3 : Coating thicknesses according temperature and feeding rate

Gas Temperature Level	Powder Feeding Rate Level	Coating Thickness (μm)
T1	3	-
T1	4	-
T1	5	33,78
T1	6	40,74
T1	7	45,83
T1	8	103,9
T1	9	124,5
T1	10	132,0
T2	3	81,2
T2	4	132,9
T2	5	138,0
T2	6	228,9
T2	7	219,4
T2	8	253,6
T2	9	309,1
T2	10	632,2
T3	3	158,2
T3	4	128,1
T3	5	173,2
T3	6	148,1
T3	7	294,4
T3	8	400,7
T3	9	563,2
T3	10	593,3
T4	3	131,9
T4	4	195,6
T4	5	275,7
T4	6	428,3
T4	7	573,1
T4	8	623,1
T4	9	910,6
T4	10	1219,0
T5	3	173,1
T5	4	274,4
T5	5	299,5
T5	6	408,1
T5	7	537,0
T5	8	1085,0
T5	9	488,4
T5	10	376,4

SEM and EDS analyses were done for investigation of bonding between K-20-11 powder and substrate. SEM analysis is given Figure 5.6 and EDS analysis is given Table 5.4.

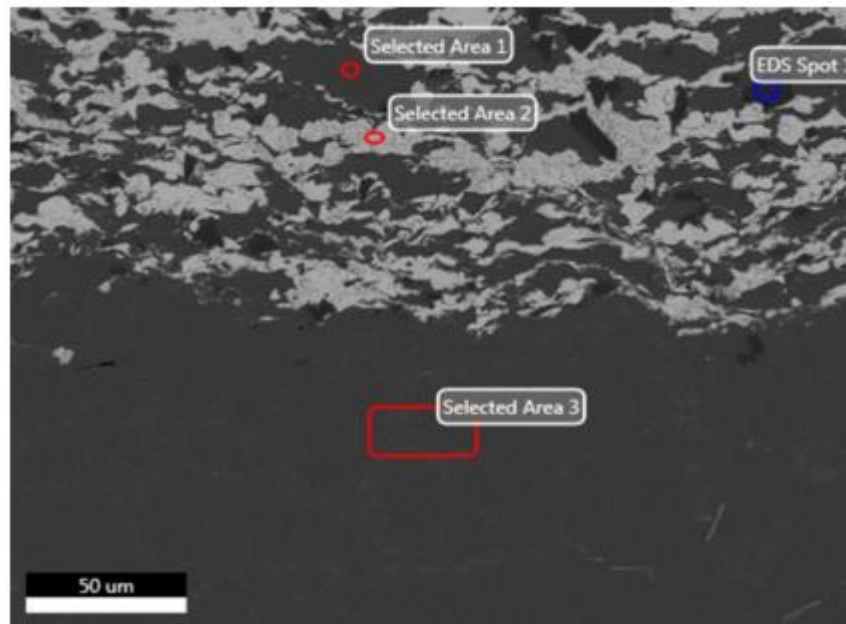


Figure 5.6 : SEM image of K-20-11 coating on A356 alloy wheel (3rd temperature level, 6th feeding rate level)

Table 5.4 : EDS analysis of K-20-11 coating on A356 alloy wheel (3rd temperature level, 6th feeding rate level)

	S. Area 1	S. Area 2	EDS Spot 1	S. Area 3
Al (Weight %)	100	2,12	54,81	88,24
Si (Weight %)	-	-	-	11,76
Zn (Weight %)	-	97,88	-	-
O (Weight %)	-	-	45,19	-

Although upper temperature steps cause oxidation and porosity problem, lower temperature steps decrease the deposition efficiency. As shown in the Table 5.3, if powder feeding rate increases, coating thickness also increases. Ozdemir et al. mentioned, powder loading on substrate increases with feeding rate under same coating conditions. Additionally they found that porosity level also increases with powder deposition [31]. Results after parameter experiments meet with this study. After defect area coated, this area will be grinded for a smooth surface. Because of this reason extensive coating is not needed and it will be additional cost for industrial applications. Additionally, while 9th and 10th feeding rate levels were using, it is realized that feeding connection pipes were stuck and coating processes was stopped. Porosity in deposition and lack of bonding between coating and substrate during high temperature and feeding rate level are shown in Figure 5.7.

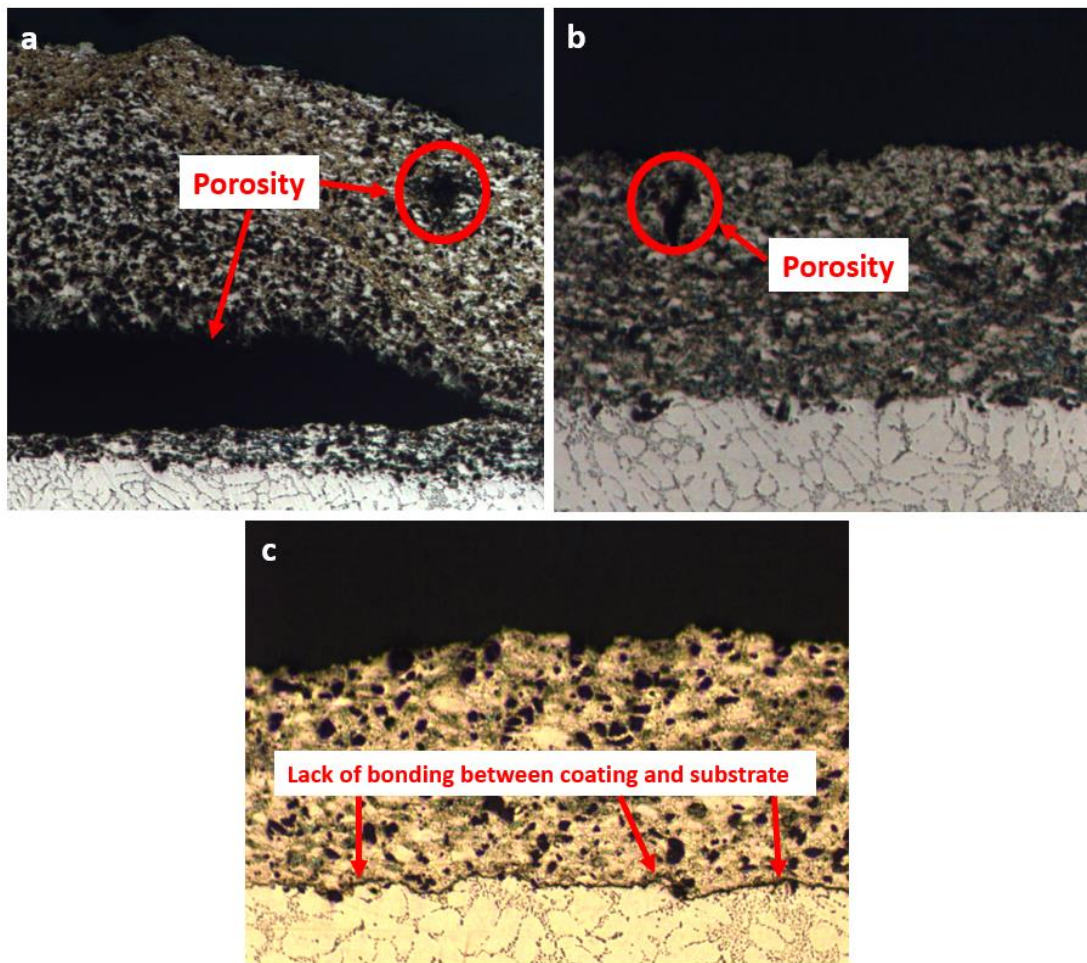


Figure 5.7 : Coating problems during high feeding rate a) 4th Temperature and 10th feeding rate level b) 5th temperature and 9th feeding rate level c) 5th temperature and 10th feeding rate level

Instead of same procedure applied for SST-A5006, stuck and non-continuous deposition occurred during coating process. At 1st, 2nd and 3rd temperature levels, generally no deposition was observed. At 4th and 5th temperature levels, in a few feeding rate levels deposition was observed. But these depositions were generally non-continuous and coatings were not smooth and homogenous. Especially in high feeding rate levels stuck was occurred many times and process was stopped. There may be several reasons for this situation;

- SST-A5006 particle size distribution is thicker than K-20-11.
- Ceramic powder absence creates stuck problem or less deposition efficiency. Winnicki et al. mentioned that the structure is similar in both cases and consists of aluminium particles, alumina particles, aluminium oxide and pores. The

presence of alumina provides high density of the coating by work hardening decreases amount of pores [30].

- As manufacturer of SST-A5006 mentioned, Dymet 423 LPCS equipment is not suitable for this powder.

For further experiments, SST-A5006 powder can be mixed with similar particle sized alumina powder, can be sieved for less particle distribution or can be used in different commercial LPCS equipments.

In Figure 5.8 SEM image and in Table 5.5 EDS analysis of SST-A5006 coating is given. It is clearly seen that porosity level is very high according to K-20-11 powder. Instead of having similar chemical composition with A356 alloy wheel, high porosity level and very less deposition efficient make SST-A5006 powder very useless for this project.

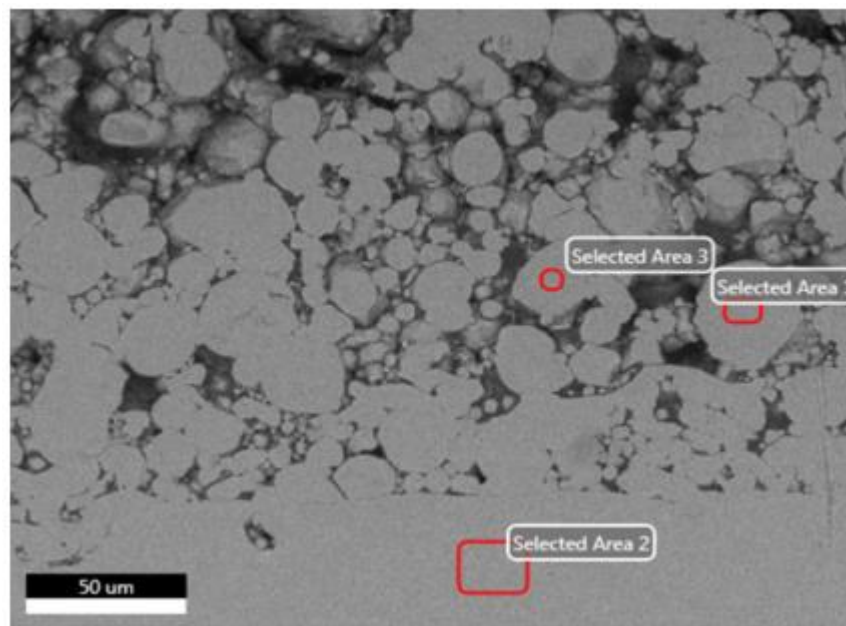


Figure 5.8 : SEM image of SST-A5006 coating on A356 alloy wheel (5th temperature level and 7th feeding rate level)

Table 5.5 : EDS analysis of SST-A5006 coating on A356 alloy wheel (5th temperature level, 7th feeding rate level)

	S. Area 1	S. Area 2	S. Area 3
Al (Weight %)	86,63	83,28	86,95
Si (Weight %)	13,37	16,72	13,05

After coating 37 wheels which have leakage defects, they were grinded for a smooth surface. Then wheels were examined in wet leakage test equipment and 36 wheels passed successfully. Just one wheel failed because of a few bubble observation. Total

scrap recover ratio is calculated as 97%. However 36 wheels pass the leakage test, mechanical performance test should be applied. After completing these tests successfully, it can be agreed on that wheels are recovered.

5.2 X-ray Control Results

The reason of X-ray controlling during wheel casting is to determine all inside casting defects such as shrinkage, gas porosity and etc. But in this section this control was applied for investigation any visible difference between A356 alloy wheel and K-20-11 coating. As Gawdzińska et al. mentioned in their study, penetration of electromagnetic wave through a complex materials such as metal matrix composites, coated or welded metal substrates [32]. It is predicted that a visible contrast difference will be seen because of density difference the powder/coating and substrate. But as it is shown in Figure 5.9, after grinding of coating the contrast difference becomes not clearly visible. If the coating is done homogenous and grinding process applied well the contrast difference can decrease more.

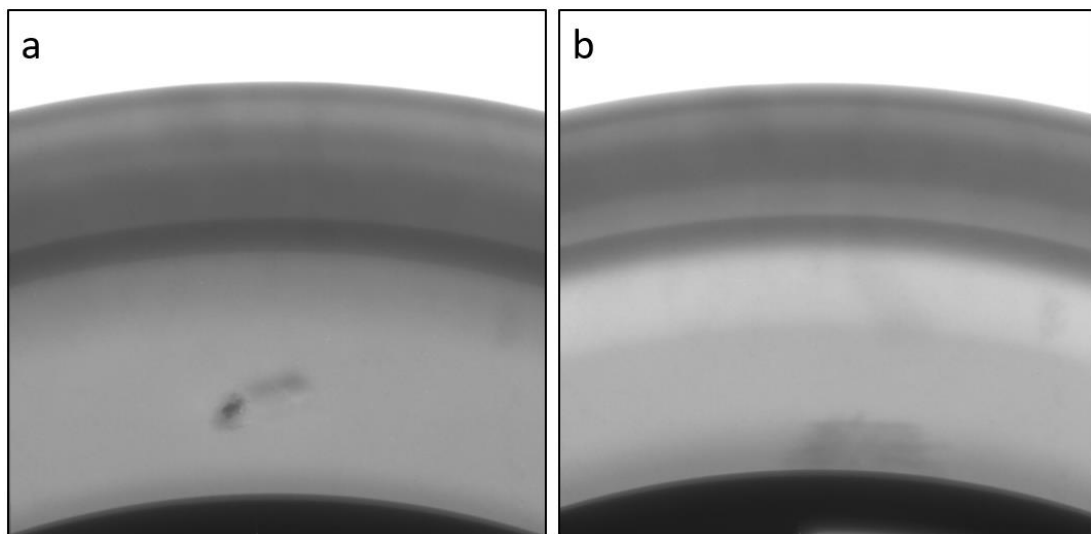


Figure 5.9 : X-ray images of rim surface a) After coating process-excessive material on rim surface b) After grinding process-smooth rim surface

If SST-A5006 powder could be successfully used in Dymet 423, there would be not any visible detection. As mentioned before, because of similar chemical composition and density X-ray units would not detect contrast difference.

5.3 Microstructure Investigation Results

After coating and grinding process, defected areas were investigated under metal microscope. As it is shown in Figure 5.10, after removing excessive deposited material stays on defected area and it is clearly seen that coating fills all leakage area.

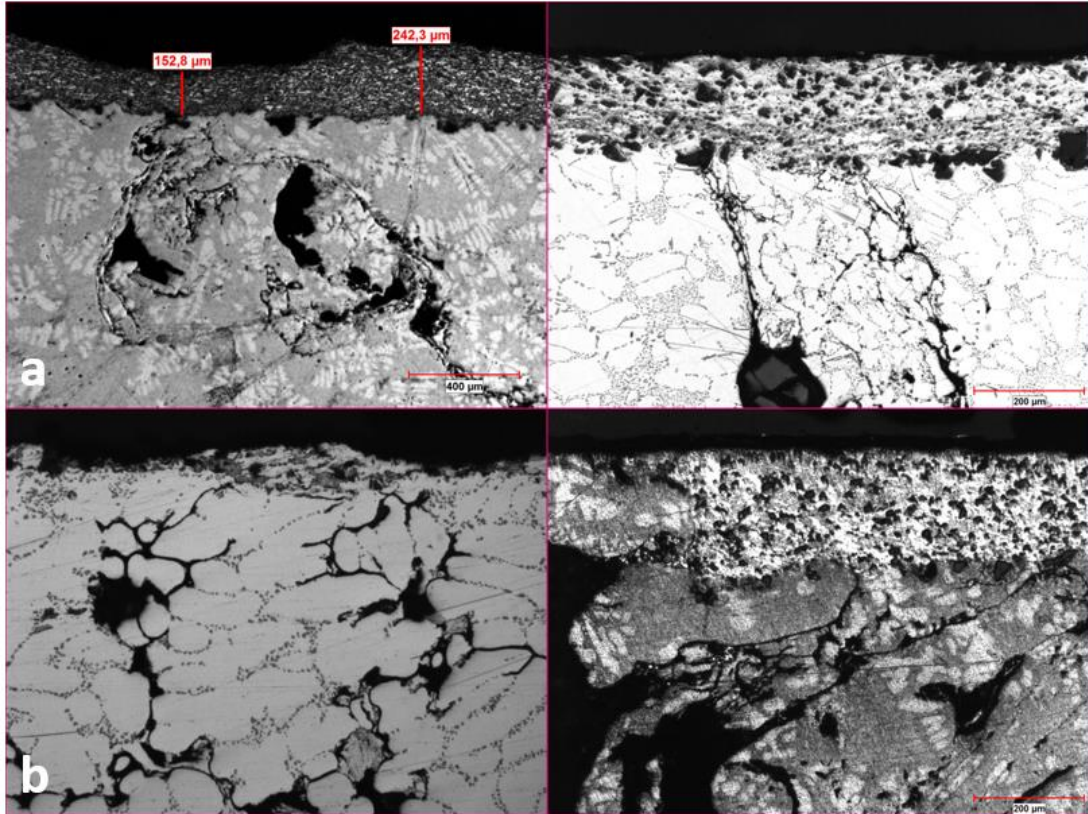


Figure 5.10 : Microstructures of coated wheel with K-20-11 a) After coating process
b) After grinding process

5.4 Hardness Test Results

All approved 36 wheels were painted after grinding process and X-ray controls. After painting process, wheels were examined for hardness. A356 wheels are mostly annealed for specific hardness and mechanical properties which are determined by customer. Coated powders are always under melting point during cold spray process instead of thermal spray processes and coating occurs in solid state [24]. For this reason hardness values are foreseen that they will not change after coating process especially defected areas.

Hardness test was done in cross section of rim surface around leakage defect zone. In every cross section part, 10 hardness measurements were done. According to customer

specifications painted wheel average hardness values should be between 80-100 HB. Randomly chosen two wheels' hardness results are given Table 5.6 and measurement zones are given Figure 5.11.

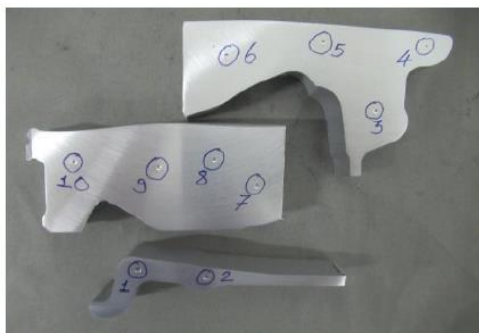


Figure 5.11 : Measurement zones for cross section Hardness Test

Table 5.6 : Hardness measurements after painting process

	Wheel No.1 HB value	Wheel No.2 HB value
Zone 1	93,00	93,80
Zone 2	87,10	88,60
Zone 3	89,00	88,30
Zone 4	90,00	93,00
Zone 5	88,60	94,30
Zone 6	81,70	89,00
Zone 7	88,30	86,00
Zone 8	91,00	87,90
Zone 9	86,40	93,40
Zone 10	87,00	87,90
Average	88,21	90,22
Judgement	OK	OK

All hardness measurements are in specification that is determined by customer. Cold spray process does not change hardness of coated area.

5.5 90° Impact Test Results

This test method is a simulation of possible impact scenario during driving through the road. Basic principle of testing method is free fall. According to customer specifications, a weight is releasing from a specific distance directly to rim surface with 90° angle. In Figure 5.12, schematic drawing of test method is given.

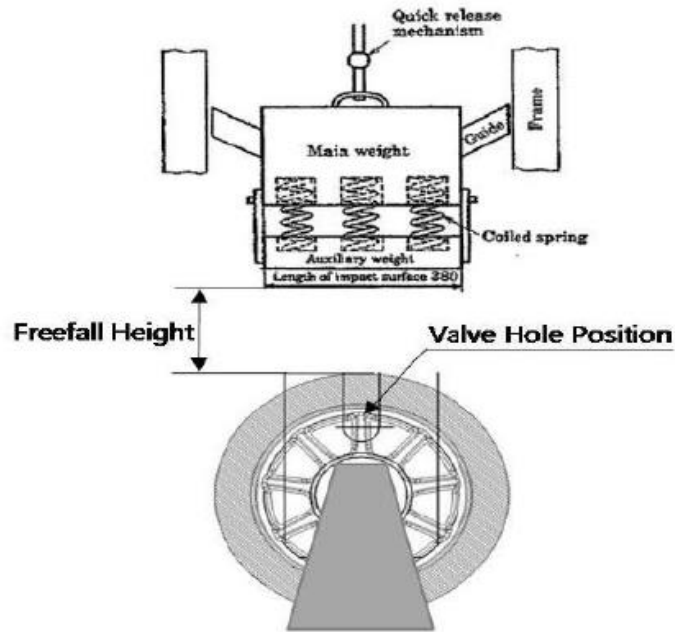


Figure 5.12 : Schematic drawing of 90° Impact Test Equipment

Test method and requirements change from every customer specification. For this reason, Wheel Model.1 and Wheel Model.2 were evaluated for their own specification. 3 different wheels were tested for each model. Wheel Model.1 results are given in Table 5.7 and Wheel Model.2 results are given in Table 5.8.

Table 5.7 : Wheel Model.1 90° Impact Test Results

	Deformation on Rim Surface		Judgement
	Spec Value (mm)	Result (mm)	
Wheel No.1	6	1,74	OK
Wheel No.2	6	2,56	OK
Wheel No.3	6	2,76	OK

Table 5.8 : Wheel Model.2 90° Impact Test Results

	Deformation on Rim Surface		Judgement
	Spec Value (mm)	Result (mm)	
Wheel No.1	Is there any complete separation on the wheel?	NO	OK
Wheel No.2		NO	OK
Wheel No.3		NO	OK

5.6 Radial Fatigue Test Results

This test method is simulation of fatigue scenario during driving through the road. Basic principle of testing method rotating the wheel under a specific load. In Figure 5.13, schematic drawing of test equipment is given.

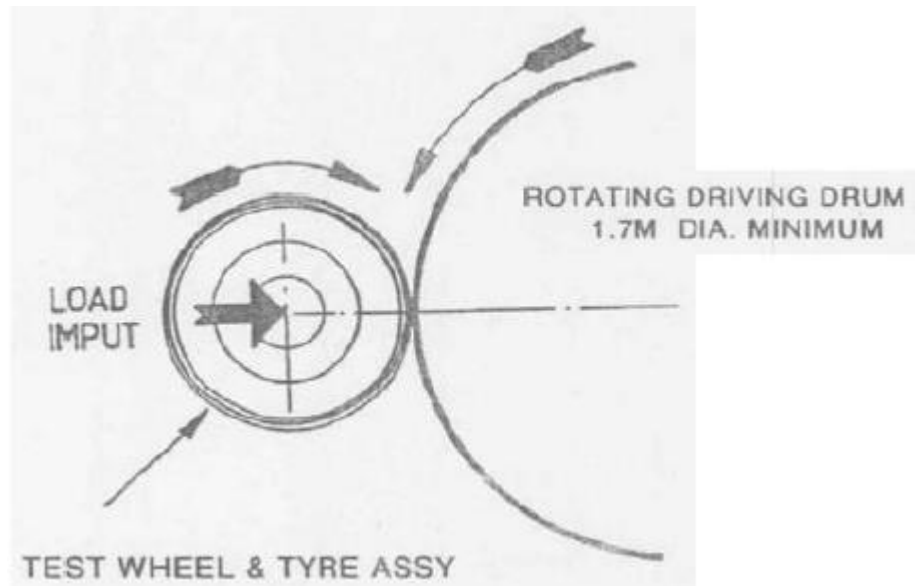


Figure 5.13 : Schematic drawing of radial fatigue test equipment

According to customer specification wheels should complete 3.000.000 cycle under momentum. Wheel Model.1 was tested under 23 kN and Wheel Model.2 was tested under 12 kN momentum. After completing 3.000.000 cycle penetration test was applied to wheels to determine crack existence. Test results are shown in Table 5.9.

Table 5.9 : Penetration test results for crack existence after radial fatigue test

	No Crack	Crack	Judgement
Wheel Model.1	X		OK
Wheel Model.2	X		OK

6. CONCLUSION

Recoverability of wheels which have leakage defects by LPCS was investigated. Two different commercial cold spray powder used as a deposition material in Dymet 423 LPCS equipment. During parameter experiments, it is clearly understood that SST-A5006 powder is not suitable for Dymet 423. Although chemical composition of this powder is similar with A356 alloy wheel, thicker particle size distribution and absence of ceramic powder blocked the feeding connections and stopped the coating process several times. For this reason commercial K-20-11 powder was chosen as deposition material to recover the wheels and coating parameters were determined as 3rd temperature level and 6th feeding rate level in Dymet 423.

37 wheels were coated on rim surface and excessive deposition was removed by grinding process. Wet leakage test was applied all coated wheels. Test result showed that 36 wheels passed successfully the leakage test and scrap recover ratio was calculated as %97.

Microstructure of coated wheel was investigated and images showed that after removing excessive material coating was still on defected areas. Very low porosity level of coating blocked defected area and prevented leakage. Although grinding process was applied on coating area, x-ray images showed that there was a nearly visible contrast difference between the substrate and coating. If SST-A5006 powder could coated, it was predicted that this contrast difference would not be seen because of similar chemical composition and density. In further experiments, particle size distribution of SST-A5006 powder can be aligned for Dymet 423 or it can be coated by more suitable LPCS equipment.

Because of safety functional requirements, mechanical performance tests were applied for the wheels. Hardness test, 90° impact test, and radial fatigue test results showed that all requirements were met according to customer requirements.

As a conclusion, all experiments and test results showed low pressure cold spray method can be used for recovering the wheels which have leakage defects. This method can be easily used in industrial scale after feasibility studies are done. Future experiments may be concentrate on recovering other casting defects such as gas holes or visual defects and can decrease scrap ratio more.

REFERENCES

- [1] Yıldırım, H. (2006). *Alüminyum malzemenin otomotiv sektöründeki uygulamaları* İstanbul Teknik Üniversitesi, İstanbul, Türkiye
- [2] Maxion Wheels Archives: Principles of Aluminium, Foundry Training Program
- [3] European Aluminium Association TALAT Lecture 1101, (1999). Resources and Production of Aluminium, Geoff Budd, Birmingham.
- [4] Apelian, D. (2009). *Aluminum Cast Alloys: Enabling Tools for Improved Performance*, NADCA
- [5] Miskovic, Z., Bobic, I., Tripkovic, S., Rac, A., and Venvl, A. (2006). The Structure and Mechanical Properties of an Aluminium A356 Alloy Base Composite With Al₂O₃ Particle Additions. *Tribology in industry*, 28, 23-26.
- [6] Maxion Wheels Archives: Melting Aluminium, Foundry Training Program
- [7] Aguirre-De la Torre, Afeltra, E., Camarillo-Cisneros, U. C. D. J., Pe´rez-Bustamante, R., and Martı´nez-Sa´nchez, R. (2013). Grain Refiner Effect on the Microstructure and Mechanical Properties of the A356 Automotive Wheels. *Journal of Materials Engineering and Performance*, 23(2), 581–587
- [8] Mattia, M., Giulio, T., Franco, B., and Gian, L. G., (2009). Impact behaviour of A356 alloy for low pressure die casting automotive wheels. *Journal of Materials Processing Technology* 209(2), 1060-1073
- [9] Maxion Wheels Archives: Molten Aluminium Treatments, Foundry Training Program
- [10] Mostafaei, M., Ghobadi, M., Eisaabadi B. G., Uludağ, M., and Tiryakioğlu, M. (2016). Evaluation of the Effects of Rotary Degassing Process Variables on the Quality of A357 Aluminum Alloy Castings. *Metallurgical and Materials Transactions B*, doi: 10.1007/s11663-016-0786-7
- [11] Hasirci, H. (2017). Advantages of produce by low pressure casting. *1st International Turkish World Engineering and Science Congress*, 593-602
- [12] Otarawanna, S. and Dahle, A.K. (2011). Casting of aluminium alloys, *Fundamentals of Aluminium Metallurgy*. Woodhead Publishing Limited, Cambridge, 141-154
- [13] Maxion Wheels Archives: Casting Defects, Foundry Training Program
- [14] Park, J. M. (2009). *Behaviours of Bifilms in A356 Alloy during Solidification: Developing Observation Techniques with 3-D Micro X-ray Tomography*, University of Birmingham
- [15] Tan, E. (2011). *Alüminyum Alaşımlarında Blister Oluşumu*. (Doctoral dissertation). Pamukkale Üniversitesi/Fen bilimleri Enstitüsü, Denizli, 21-32
- [16] Karthikeyan, J. (2004). Cold spray technology:International status and USA efforts, report by ASB Industries
- [17] Choudhuri, A., Mohanty, P.S., and Karthikeyan, J. (2015). Bio-ceramic Composite Coatings by Cold Spray Technology. *Proceedings of the International Thermal Spray Conference*, doi:10.1361/cp2009itsc0391.

- [18] Papyrin, A. (2001). Cold spray produces high quality coatings for a wide spectrum of applications. *Advanced Materials & Processes*, 49-51
- [19] Irissou, E., Legoux, J., Ryabinin, A. N., Jodoin B., and Moreau, C. (2008). Review on Cold Spray Process and Technology: Part I—Intellectual Property. *Asian Journal of Engineering and Applied Technology* 5(1), 1-3
- [20] Ghelichi, R. and Guagliano, M. C. (2009). Coating by the Cold Spray Process: a state of the art. *Frattura ed Integrità Strutturale* 8, 30-44
- [21] MOOG Aircraft Group, (2018). Cold Spray Repair Services
- [22] Kashirin, A., Klyuev, O., Buzdygar, T., and Shkodkin, A. (2011). Modern Applications of the Low Pressure Cold Spray
- [23] Arbegast Materials Processing and Joining Lab, (2012). Cold Spray: A guide to best practice
- [24] Singh, H., Sidhu, T.S., and Kalsi, S.B.S. (2012). Cold spray technology: future of coating deposition processes. *Frattura ed Integrità Strutturale* 22, 69-84
- [25] Papyrin, A., Kosarev, V., Klinkov, S., Alkimov, A., and Fomin, V. (2007). Current status of the cold spray process, *Cold Spray Technology*, 248-323
- [26] Yin, S., Cavaliere, P., Aldwell, B., Jenkins, R., Liao, H., Li, W., and Lupoi, R. (2018). Cold spray additive manufacturing and repair: fundamentals and applications. *Additive Manufacturing*, doi: 10.1016/j.addma.2018.04.017
- [27] Altuncu, E. and Ustel, F. (2017). Soğuk sprej teknolojisi ve uygulama alanları. *Metalurji* 157, 29-40
- [28] Moridi, A., Hassani-Gangaraj, S. M., Guagliano, M., and Dao, M. (2014). Cold spray coating: review of material systems and future perspectives. *Surface Engineering* 36(6), 369-395
- [29] Winnicki, M., Piwowarczyk, T., Malachowska, A., and Ambroziak, A. (2014). Effect of gas pressure and temperature on stereometrics properties of Al+Al₂O₃ composite coatings by LPCS method. *Archives Of Metallurgy And Materials* 59(3), 879-886
- [30] Winnicki, M., Malachowska, A., Piwowarczyk, T., Rutkowska-Gorczyca, M., and Ambroziak, A. (2016). The bond strength of Al + Al₂O₃ cermet coatings deposited by low-pressure cold spraying. *Archives of Civil and Mechanical Engineering* 16(4), 743-752
- [31] Ozdemir, O. C., Widener, O. C., Carter, M. J., and Johnson, K. W. (2017). Optimization of Particle Feeding Rates in High Pressure Cold Spray Systems
- [32] Gawdzińska, K., Grabian, J., and Przetakiewicz, W. (2008). Use Of X-Ray Radiography In Finding Defects In Metal-Matrix Composite Casts. *Metalurgija* 47(3), 199-201

APPENDIX

APPENDIX A

K-00-04-16 Material Safety Data Sheet

Material Safety Data Sheet

Aluminum oxide powder

Creation date January 10, 2008

Section 1 - Product Identification

Product class: Aluminum oxide powder
Trade name: Powder K-00-04-16
Synonyms: None.
Manufacture's name: OCPS Ltd.
Address: ul. Kurchatova, 21, Obninsk, Kalujskaya oblast, 249031, RUSSIA
Phone: +7 (48439) 68007

Section 2 - Composition, Information on Ingredients

Chemical characterization.

Description: Simple substance powder listed below.

CAS#	Chemical Name	Wt, %	Hazardous
1344-28-1	ALUMINUM OXIDE (99.4% purity)	100	Yes

Section 3 - Hazards Identification

EMERGENCY OVERVIEW

WARNING! May irritation to skin, eyes and respiratory tract.

J.T. Baker SAF-T-DATA[™] Ratings (Provided here for your convenience)

Health Rating: 1 - Slight

Flammability Rating: 0 - None

Reactivity Rating: 0 - None

Contact Rating: 1 - Slight

Potential Health Effects

Inhalation:

Hazard is principally that of a nuisance dust. Coughing or shortness of breath may occur in cases of excessive inhalation.

Ingestion:

No adverse effects expected.

Skin Contact:

Causes irritation to skin.

Eye Contact:

No adverse effects expected but dust may cause mechanical irritation.

Chronic Exposure:

No adverse effects expected.

Aggravation of Pre-existing Conditions:

Not expected to be a health hazard.

Section 4 - First Aid Measures

Eyes:

Flush eyes with plenty of water for at least 15 minutes, occasionally lifting the upper and lower eyelids. Get medical aid if irritation persists.

Skin: Flush skin with plenty of soap and water for at least 15 minutes while removing contaminated clothing and shoes. Get medical aid if irritation develops or persists.

Inhalation: Remove to fresh air. Get medical attention for any breathing difficulty.

Ingestion: Give several glasses of water to drink to dilute. If large amounts were swallowed, get medical advice.

APPENDIX B

K-20-11 Material Safety Data Sheet

Material Safety Data Sheet

Aluminum oxide powder – Aluminum powder – Zinc powder mixture

Creation date June 28, 2006

Section 1 - Product Identification

Product class: Aluminum oxide powder - Zinc powder mixture
Trade name: Powder K-20-11
Synonyms: None.
Manufacturer's name: OCPS Ltd.
Address: ul. Kurchatova, 21, Obninsk, Kalujskaya oblast, 249031, RUSSIA
Phone: +7 (48439) 68007

Section 2 - Composition, Information on Ingredients

Chemical characterization.

Description: Mechanical mixture of simple substance powders listed below.

CAS#	Chemical Name	Wt, %	Hazardous
1344-28-1	ALUMINUM OXIDE (99.4% purity)	23-27	Yes
7429-90-5	ALUMINUM	33-37	Yes
7440-66-6	ZINC(96% purity)	38-42	Yes

Section 3 - Hazards Identification

EMERGENCY OVERVIEW

Aluminum and zinc components of the powder mixture react with water and slowly generate heat and hydrogen gas which can form explosive mixtures in air.

Potential Health Effects

Inhalation:

Coughing or shortness of breath may occur in cases of excessive inhalation. If user operations generate zinc oxide fume, inhalation of the fume can result in metal fume fever. Can cause mild irritation of the throat.

Ingestion: If ingested, powder may produce irritation of the digestive tract and diarrhea.

Skin Contact: Causes mild irritation to skin.

Eye Contact: Powder may cause mechanical irritation.

Chronic Exposure: Repeated inhalation can cause chronic respiratory disease.

Aggravation of Pre-existing Conditions: Pre-existing upper respiratory and lung diseases such as, but not limited to: Bronchitis, Emphysema and Asthma.

Section 4 - First Aid Measures

Eyes: Flush eyes with plenty of water for at least 15 minutes, occasionally lifting the upper and lower eyelids. Get medical aid if irritation persists.

Skin: Flush skin with soap and water while removing contaminated clothing and shoes. Get medical aid if irritation persists.

Swallowed: Let the person rinse the mouth and vomit by inserting fingers into the throat. Get medical aid.

Inhalation: Remove from exposure to fresh air immediately. If not breathing, give artificial respiration. If breathing is difficult, give oxygen. Get medical aid.

Section 5 - Fire Fighting Measures

Fire, explosion: Mixture is considered to be moderately flammable and explosive by heat or flame. Aluminum and zinc components of the powder mixture react with water and generate hydrogen gas, which can form explosive mixtures in air.

Extinguishing Media: DO NOT use water or halogenated extinguishers. Use dry sand to cover and ring the burning powder.

Special Information: Use protective clothing and breathing equipment appropriate for the surrounding fire and to protect against the dust that may be dispersed in the air.

APPENDIX C

SST-A5006 Technical Data Sheet



SST-A5006

PRACTICAL COLD SPRAY COATINGS

Document No: SST-TDS-A5006-PR-1.1-0415
Release Date: April 2015

TECHNICAL DATA SHEET

Document No: SST-TDS-A5006-PR-1.1-0415
Release Date: April 2015



Commercial Powder

Metal Group – ALUMINUM
Catalogue No. – SST-A5006



Description:

Aluminum Silicon Alloy powder (AA4047, SST Catalog No. SST-A5006) with special particle size distribution for cold spray processes with general applications in salvage and restoration of aluminum and magnesium components. The cold spray coating presents high density, excellent bonding strength on magnesium alloy substrate, and good machinability.

Specifications:

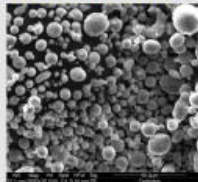
Material Properties

Composition: **Al12Si 99% Min.**
Particle Size: **-45 to +5 µm**
Characteristics: **Spherical particles**

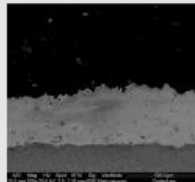
Typical Coating Properties

Bond Strength: **> 9500 psi**
Deposition Efficiency: **Up to 27% (with powder heater)**
Deposition Rate: **Up to 10 g/min**
Hardness (Brinell): **89 – 97**
Density: **> 97%**

Typical Micrograph



SST-A5006 Powder



SST-A5006 Coating on
Mg alloy (Series EP)

Ordering Information

Catalogue Number: **SST-A5006**
Standard Packaging: **400 ml or 1 gallon sized container**
Selling Unit: **Pound**
Material Certification: **Available upon request**

Recommended Spray Parameters

(when utilizing CenterLine Cold Spray equipment. Recommendations may not apply when making use of non-CenterLine equipment)

Series EP

Temperature: **450 – 500°C**
Pressure: **450 – 500 psi**
Powder Pre-heating*: **≤ 350°C**
Standoff Distance: **10 – 40 mm**
Gas: **Nitrogen**
Feed Rate (gram/min.): **12 – 50**
Gun Traverse Speed: **10 – 200 mm/s depending on process settings and target coating thickness**
Surface Preparation: **SST-G0002 commercial blast or grease free as-machined surface**
Spray Nozzle: **UltiFlow™**

To discuss your Cold Spray Application(s) or for more information about powders and blends, please contact your CenterLine SST representative or visit our website at www.supersonicspray.com.

* Notice for Powder Heater Use

Due to the specific material characteristics of this powder, equipment settings that deviate from the **Recommended Spray Parameters** listed above may result in clogging the powder heater. These parameters are based on 10 minutes of continuous spray time. For applications that require continuous spray times exceeding 10 minutes, please consult with CenterLine to receive assistance in optimizing spray parameters. Note that the SST Spray Machine and Gun User's Manuals also contain information on proper settings and operating parameters.

CenterLine (Windsor) Limited, Supersonic Spray Technologies Div., 655 Morton Drive, Windsor, ON, N9J 3T9,
Phone: (519) 734-8330, Toll Free: (800) 268-8330,

Email: info@cntrline.com, website: www.supersonicspray.com

©2015 CenterLine (Windsor) Limited

CURRICULUM VITAE

SAMET YILMAZ

Villakent Mahallesi, Menemen/IZMIR, Mobile: +90 544 520 8188, e-mail: sametyilmaz89@gmail.com

PERSONAL INFORMATION

Marital Status : Single
Nationality : T.C.
Military Service : Completed (Discharge Date: 17/07/17)
Date of Birth : 29/05/1989
Place of Birth : Manisa/ Soma
Driving License : B



EDUCATION

Master of Science İzmir Katip Celebi University
2014 – 2019 Material Science Engineering

Bachelor's Degree İstanbul Technical University
2007 – 2012 Metallurgical and Materials Engineering

High School Karşıyaka Anatolian High School
2003 – 2007

WORK EXPERIENCES

Maxion Wheels Aluminium
04.2018 – ...

Process Quality Engineer

- Leading Casting Quality Team
- Raw Material Inspection
- Responsible for Material Lab.
(Chemical Composition, Density and Hardness Analyses)
- Responsible for Visual Controls
- Responsible for X-ray Controls
- Management of Scrap Materials

Eldor Izmir
09.2017 – 04.2018

Incoming Quality Engineer

- Incoming quality controls of raw materials
- Detection and Investigation of Nonconformities
- Nonconformity Reports
- Nonconformity Costs

Sentes-Bir A.Ş

Quality Control and R&D Engineer

04.2013 – 02.2017

Quality Control:

- Leading Quality lab.
- Spectral Analyses of Nickel, Copper and Iron based materials
- Sieve and oxygen content analyses of powder materials
- Microstructure analyses
- HRC, HV, HB hardness analyses
- Customer quality control reports
- ISO 9001 and ISO TS 16949 documentation
- APQP/PPAP, MSA, SPC, DFMEA and FMEA preparation

R&D:

- TEYDEB, KOSGEB, SANTEZ project designs
- Carrying out R&D and P&D projects

Meta-Mak A.Ş

Sales & Marketing Assistant

09.2012 – 04.2013

- Spare part selling and marketing
- Fair organizations

INTERNSHIP INFORMATIONS

- **İSFALT** *04.2012 – 05.2012*
It is done for the thesis project which is called "Investigation of electrical arc furnace slags as an asphalt aggregates"
- **Prof. Dr. Adnan Tekin**
Malzeme Uyg-Ar Merkezi *08.2011 – 09.2011*
- **CMS Jant ve Makina A.Ş** *06.2011 – 07.2011*
- **İzmir Demir Çelik San. A.Ş** *06.2010 – 07.2010*

SKILLS

Software :

Microsoft Office, Tableau, SAP, Fortran, Catia, Solidworks, HSC, Factsage, PANalytical X'Pert HighScore Plus(XRD Analyses), Faris (X-ray)

Foreign Language:

English (Fluent), German (Beginner)

Certificates:

- Failure Mode Effect Analysis (FMEA)Training Course, IATF Cert No:5-ADP-12-05-1820
- ISO/TS 16949 Training Course, IATF Cert No:5-ADP-12-05-1820
- Internal Auditor Training Course, IATF Cert No:5-ADP-12-05-1820
- Statistical Process Control (SPC), IATF Cert No:5-ADP-12-05-1820

- Measurement System Analysis (MSA), IATF Cert No:5-ADP-12-05-1820
 - APQP & PPAP Training Course, IATF Cert No:5-ADP-12-05-1820
 - Solidworks Training Course, TEGEP
 - X-Ray Control Training, Bossello
 - Glow Discharge-OES Training Course, HORIBA
 - 6 Sigma - Yellow Belt, SPAC
-

PUBLICATIONS & PRESENTATIONS

- **Yılmaz S., Ozdemir I.** Wear Plate Production By Clad Brazing Method 11-13 May 2016, 4th International Conference on Welding Technologies and Exhibition (ICWET'16), Gaziantep-TURKEY (Oral Presentation)
 - **Çelik E., Yılmaz S.** Mekanik Olarak Alaşımlandırılmış Fe-Co-Cu Alaşım Tozlarının ve Hidrometalurjik Olarak Üretilmiş Metal Tozlarının Mekanik Özelliklerinin Karşılaştırılması, 2014, 7th International Powder Metallurgy Conference and Exhibition (Poster Presentation)
 - **Çelik E., Yılmaz S.** Su Atomizasyonu İle Üretilmiş Fe Esaslı Alaşım Tozların Elmaslı Kesici Takımlarda Kullanılabilirliği, 2014, 7th International Powder Metallurgy Conference and Exhibition (Poster Presentation)
 - **Yılmaz S., Ünal A., Yücel O.** An Investigation on EAF Slag Treatment, IISS 2012 International Iron & Steel Symposium, April 2 - 4, Karabük (Poster Presentation)
 - **Yılmaz, S., Alkan M., Yücel O., Derin B.** Production of ZrB₂ Powders from ZrO₂ Containing Dental Implant Wastes, 2012, TMS Annual Meeting & Exhibition, March 11-15, Orlando, Florida (Oral Presentation)
-

PROJECTS

- Production of ZrB₂ from ZrO₂ Dental Implant Wastes by Self-Propagating High Temperature Synthesis (SHS), TÜBİTAK BİDEB 2209, 2011-2012
-

ORGANIZATIONS

- 17th International Symposium on Boron, Borides and Related Materials – ISBB (Organization Committee)
-

REFERENCES

Available on request.
